Deliverable D4.1

Papers submitted by the PhD candidate

Project acronym	Academics4Rail
Starting date	01.09.2023
Duration (in months)	42
Call (part) identifier	HORIZON-ER-JU-2022-02
Grant agreement no	101121842
Due date of deliverable	31.08.2025
Actual submission date	28.08.2025
Code	D4.1
Responsible/Author	Stefano Bruni
Dissemination level	Public
Status	Final

Europe's Rail
Co-funded by the European Union

Funded by the European Union. Views and opinion expressed are however those of the author(s) only and do not necessarily reflect those of the European Union or the Europe's Rail Joint Undertaking. Neither the European Union nor the granting authority can be held responsible for them. The project Academics4Rail is supported by the Europe's Rail Joint Undertaking and its members.

Document history		
Revision	*Date*	*Description*
1	28.08.2025	Prefinal version

Report contributors		
Name	Beneficiary Short Name	Details of contribution
Stefano Bruni	PMI	Overall management, supervision of the PhD candidate
PaoloSchito	PMI	Co-supervision of the PhD candidate, support to CFD analyses
James Bell	DLR	State-of-the-art analysis, support to the PhD candidate
Arne Henning	DLR	State-of-the-art analysis, support to the PhD candidate
Joao Pombo	HUD	State-of-the-art analysis, support to the PhD candidate
Ariane Wettig	TUB	State-of-the-art analysis, support to the PhD candidate

Contents

1 Executive Summary 4

2 Status of research work of the PhD candidate 5

3 Papers submitted by the PhD candidate 6

4 Conclusions 8

Appendix A: paper "Aerodynamics of Freight Trains: An Open Database of Geometries for CFD Analyses" 9

Appendix B: paper "A review of freight trains aerodynamics" 25

Appendix C: paper "Aerodynamics of Freight Trains: addressing the complexity of train geometry through an open database" 80

Abbreviations and acronyms

DoA	Description of the Action

1 Executive Summary

This document is an interim version of deliverable D4.1 and provides a concise report of the research performed so far by Luca Corniani, the PhD candidate hired by Politecnico di Milano (PMI) to carry out research work about aerodynamics of freight trains.

The report also provides the present (August 2025) status of publications produced by the candidate and submitted to international scientific journals. So far, the candidate produced the following publications:

1. one conference paper, presented by the candidate at the Sixth International Conference on Railway Technology: Research, Development and Maintenance “Railway 2024”, held in Prague, Czech Republic, in September 2024;
2. one paper providing a State-of-the-Art review about freight train aerodynamics, submitted to the international journal “Proceedings of the Institution of Mechanical Engineers, Part F: Journal of Rail and Rapid Transit”, which is presently under second review;
3. one paper presenting the database of freight train geometries and its use for the study of freight train aerodynamics, which is going to be submitted not later than September 5th 2025 to the international journal “Promet - Traffic & Transportation Journal”.

Additionally, the student prepared a database of freight train geometries which is made available in open form to the entire scientific community in a public GitHub repository.

2 Status of research work of the PhD candidate

The PhD candidate, Mr. Luca Corniani, was hired by Politecnico di Milano (PMI) through a competitive examination and started his position as PhD Candidate on September 1st 2023, so he is now entering the third year of his PhD.

Prof. Stefano Bruni was appointed as the main supervisor of the candidate, with Prof. Luca Schito being the co-supervisor and Prof. Andrea Manes being the Tutor.

The candidate has attended all the courses that constitute his educational obligations in line with requirements for Doctoral studies at Politecnico di Milano. These consist of 4 courses for a total of 21 credits, out of which two courses (10 credits) devoted to transferable skills and the other two courses (11 credits in total) devoted to acquiring specific skills related to computational and experimental fluid dynamics. The candidate withstood so far the final examination for 3 out of these 4 courses and acquired the corresponding credits. The final examination for the remaining course is expected to take place in September 2025. Table 1 reports the titles of the courses, the status of the final examination and the grade obtained.

The PhD candidate spent a 2-week short stay at the University of Huddersfield, one of the partners of WP4. During the stay, he had the opportunity to visit the university's research facilities for railway engineering and to discuss with experts at HUD the issue of geometry defeaturing which is highly relevant to the definition of CFD models looking for a trade-off between accuracy and computational effort.

Mr. Corniani is now spending a long stay, with foreseen duration 3 to 4 months at DLR in Goettingen (in line with the plans foreseen in the DoA, see *Subtask 4.2.3: Visiting scholars*). In this stay, he is arranging and performing wind tunnel tests to gather experimental results which will be used for the validation of CFD models for freight trains, considering in particular the effect of gaps between containers in intermodal container trains.

Table 1 – Courses in the study plan of the PhD candidate

COURSE TITLE	Type (T=transferable; S=specific)	Grade	Credits	Date / Expected date
Research skills	T	30/30 cum laude	5	18-06-2024
Science, technology, society and Wikipedia	T	29	5	18-09-2024
Computational fluid-dynamics with open-source software	S	30/30 cum laude	5	14-07-2024
Aerodynamics of transport vehicles	S		6	30-09-2025

The progress of the candidate is being formally assessed by means of periodic meetings with a panel of professors who are members of the faculty of the PhD course in Mechanical Engineering at Politecnico di Milano. These periodic meetings are held annually, and therefore the candidate withstood so far two examinations:

1. the 12 months examination, held on 05-09-2024;
2. the 24 months examination, held on 24-07-2025.

in both these examinations the candidate was awarded with the grade “B” which is, according to the rules of Politecnico di Milano, the second-highest evaluation, with the highest reserved to the top 5% candidates and very seldom awarded in the first year.

With respect to the plans reported in the DoA, which were foreseeing the periodic assessment of the candidate by means of six-monthly meetings, it should be noted that this was based on the rules in force at the Department of Mechanical Engineering of PMI for the assessment of PhD candidates at the time when the DoA was prepared, but these rules were recently modified and now foresee the assessment by means of 12-monthly meetings.

The progress of the candidate was also assessed by representatives of all WP4 partners, through online meetings, which are being regularly held throughout the entire duration of the WP.

3 Papers submitted by the PhD candidate

The overall plan of publications for the candidate foresees 2 papers presented at international conferences and 3 papers published in international journals. In more detail:

1. **Conference paper n. 1**, entitled *Aerodynamics of Freight Trains: An Open Database of Geometries for CFD Analyses* presents a summary of the work performed in SubTask 4.1.1 of the project “Database of freight wagon geometries”. This paper was already presented by Mr. Corniani at the Sixth International Conference on Railway Technology: Research, Development and Maintenance and is **published in the conference’s proceedings**, with doi:10.4203/ccc.7.3.20. The full paper is reported in Appendix A of this report;
2. **Conference paper n. 2**, entitled *Numerical investigation of freight train aerodynamics: towards greener freight transport in Europe* is **in preparation** and it is hoped that it will be selected for presentation at the International Conference Transport Research Arena 2026, to be held in Budapest on May 18-21 2026;
3. **Journal paper n.1**, entitled *A review of freight trains aerodynamics*, presents the results of a detailed analysis of the State-of-the-Art performed by the candidate as the initial part of his work in SubTask 4.1.2. This paper has been submitted to the Proceedings of the Institution of Mechanical Engineers, Part F: Journal of Rail and Rapid Transit (https://journals.sagepub.com/home/pif). The article is presently **under second review,** and it is hoped that it will soon be accepted for publication. The revised manuscript submitted to the journal for the second review is reported in Appendix B of this report;
4. **Journal paper n.2**, entitled *Aerodynamics of Freight Trains: addressing the complexity of train geometry through an open database*, presents in detail the result of work done in SubTask 4.1.1 and some initial results from SubTask 4.1.2. This paper **will be submitted not later than September 10th 2025** for a special issue of the international journal “Promet - Traffic & Transportation Journal” (https://trafficandtransportation.fpz.hr/home). The final draft of this manuscript is reported in Appendix C of this report;

5. **Journal paper n.3**, title to be defined, is presently **in preparation** and will describe the final results of SubTask 4.1.2, i.e. the validation of freight train CFD models and guidelines for CFD modelling of freight trains. No draft of this manuscript is attached to this report, as the preparation of this paper is still in progress.

In case time allows, the preparation of another paper, either for a conference or for submission to an international journal will be targeted, with the contents of this final paper addressing the analysis of aerodynamic effects on freight trains, in line with the contents of SubTask 4.1.3.

4 Conclusions

In conclusion, it can be stated that the work of the PhD candidate in WP4 is progressing in line with the plans reported in the DoA. The work of the candidate was carefully supervised both by the internal supervisor, co-supervisor and tutor at PMI and by representatives of all WP4 partners through periodic online meetings.

The minimum scientific output expected from the candidate as stated in the DoA (at least one conference paper presented and one paper submitted to international scientific journals) has already been achieved, and the candidate is pursuing a more ambitious plan that can realistically lead to the publication of two conference papers and at least 3 papers published in international scientific journals.

Appendix A: paper “Aerodynamics of Freight Trains: An Open Database of Geometries for CFD Analyses”

This paper was presented at the Sixth International Conference on Railway Technology: Research, Development and Maintenance and is published in the conference’s proceedings, with doi:10.4203/ccc.7.3.20

The full bibliographic reference of the paper is:

L. Corniani, P. Schito, S. Bruni, "Aerodynamics of Freight Trains: An Open Database of Geometries for CFD Analyses", in J. Pombo, (Editor), "Proceedings of the Sixth International Conference on Railway Technology: Research, Development and Maintenance", Civil-Comp Press, Edinburgh, UK, Online volume: CCC 7, Paper 3.20, 2024, doi:10.4203/ccc.7.3.20.

In the next pages, the full paper is reported.

Proceedings of the Sixth International Conference on
Railway Technology: Research, Development and Maintenance
Edited by: J. Pombo
Civil-Comp Conferences, Volume 7, Paper 3.20
Civil-Comp Press, Edinburgh, United Kingdom, 2024
ISSN: 2753-3239, doi: 10.4203/ccc.7.3.20

Aerodynamics of Freight Trains: An Open Database of Geometries for CFD Analyses

L. Corniani, P. Schito and S. Bruni

Department of Mechanical Engineering, Politecnico di Milano
Italy

Abstract

The computational investigation of freight train aerodynamics requires the production of a surface geometry of the vehicle in order to run the simulation. To address the need for efficient production of these geometries that comes with the growing employment of numerical studies in this field, a database of representative wagon and locomotive geometries is proposed in this work.
After the database is introduced, a demonstrational computational fluid dynamics study is presented, considering the geometry of a single flat wagon with a container for two different levels of detail, and the results of the simulations are compared and discussed.

Keywords: train aerodynamics, freight trains, database, container, computational fluid dynamics, URANS.

1 Introduction

The strategic European goal to shift the long-distance-transport of goods from road to rail necessitates the eventual increase in the speed of freight trains to at least 160 km/h (Geischberger et al. [1]). At this speed, the aerodynamic effects that are mostly negligible at lower speeds become highly relevant.

Aerodynamic forces grow approximately with the square of the velocity of the flow, thus increasing the train speed resulting in greater aerodynamic forces on the vehicle. Research from Quazi et al. [2] and Alam et al. [3] shows that freight trains encounter wind from yaw angles mostly below 20°, and therefore the main component

of the aerodynamic force on a moving train is drag. This means that the increase of service speed has direct consequences for the cost and environmental impact of the operation of the train, since the mechanical power spent by the locomotive is proportional to the overall resistance to motion. Other components of the force are also of interest, since both lift and side force generate overturning moment on the wagons and must be contained to reduce the risk of derailment.

A subject of intense study directly linked to drag is the effect of empty wagons and of the size of gaps between containers, Maleki et al. [4] showed that the pressure component of drag is closely related to the size of the gap between containers. Additionally, slipstream velocities generated by a freight train tend to increase for larger gaps (Flynn et al. [5] and Li et al. [6]), in the absence of crosswind, these velocities are not sufficient to put a person stability at risk, but crosswind amplifies this effect enough to destabilize large portions of the population (Flynn et al. [7]).

Unlike streamlined passenger trains, freight trains behave as bluff-bodies and thus the flow around these vehicles is more turbulent and intrinsically unsteady. The study of freight train aerodynamics is further complicated by the fact that they can be composed of a variety of wagons with diverse geometries. These differences between passenger and freight trains call for an investigation of the flow around the latter as a separate endeavour.

The aerodynamics of freight train has been studied in the literature with both numerical and experimental methods, complementing each other with their relative strengths and drawbacks. Experimental methods measure pressure and flow velocity directly and therefore are inherently more reliable than numerical methods, however, they are also much more expensive and time-consuming.

Most experimental studies on freight trains are conducted in wind tunnels. Alam et al. [8] performed a wind tunnel test on a 1:15 model scale of a double stacked container wagon in isolation; subsequent studies by Giappino et al. [9], Kocon et al. [10] and Alam et al. [3] focused on the risk of overturning caused by crosswind on freight wagons and concluded that the relative aerodynamic coefficients are larger at high yaw angles (although a train is unlikely to encounter such angles while in motion). Wind tunnel tests have also been used by Soper et al. [11] and Sterling et al. [12] to study the slipstream velocities generated by freight trains and found them to be much greater than what was observed in passenger trains. Intermodal transport of freight has also been the subject of wind tunnel tests. Giappino et al. [13] tested different train configurations with different gap sizes and concluded that for each wagon, the best condition (both in terms of drag and overturning moments) is to be preceded by a loaded wagon and followed by an empty one. This is true for the single wagon, however, whilst for the purpose of minimizing the drag for the entire train smaller gap sizes are to be preferred, as shown based on wind tunnel tests by Soper et al. [14] and on CFD by Maleky et al. [4].

In all wind tunnel experiments that involve freight trains, the Reynolds number of the test is much lower than in full-scale experiments and this makes the latter more reliable, however the former is still often preferred for the lower costs also considering that for Reynolds numbers greater than $2.5 \cdot 10^5$ the aerodynamic coefficients become insensitive to Reynolds number (Bocciolone et al. [15]). Soper et al. [16] used full-scale experiments to compare the aerodynamics of passenger and freight trains and

found that freight trains at low speed generate slipstream velocities higher than the passenger trains, although not in violation of the TSI regulations (it should however be noticed that numerical investigations by Flynn et al. [7] found that in cases of crosswinds at a yaw angle of 30° the slipstream velocities produced by freight trains even at moderate velocities were in violation of the TSI limits for faster trains). The measurement of a full-scale underbody flow has been used by Soper et al. [17] to conclude that on well-maintained tracks the aerodynamic forces on ballast and the inertial ones due to track displacement are comparable, but poorly maintained tracks may increase the risk of ballast flight significantly.

Numerical studies allow to evaluate the flow in every point of the domain; however, the results are also affected by the physical modelling of the problem, and one of the most significant decisions to make in CFD is the modelling method for turbulence.

Different works have been published comparing the accuracy and cost of different methods (Wang et al. [18], Wang et al. [19] and Maleki et al. [20]) and they agree on the fact that RANS and URANS are unsuitable for the simulation of freight trains because of the pronounced unsteadiness of the flow. The expensive LES (or more often in recent works ELES, DES or DDES) are generally agreed to be the most accurate methods, predicting flow topology and aerodynamic coefficients in line with experimental results. It should be noted however, that while RANS methods fail to predict the numerical value of aerodynamic coefficients, they predict their trends and are suitable for comparing the performance of different geometries (Maleki et al. [20]).

The Academics4Rail research project, funded by the European community under the Europe's Rail funding programme, has launched a comprehensive investigation on the aerodynamics of freight trains. The objective is to define guidelines for the creation of CFD models of freight trains, analyse different realistic operation scenarios and synthesise the results in guidelines for safer and more efficient operation of freight trains in regard of aerodynamic effects.

Given the breadth of the problems addressed, the need for the efficient definition of geometric models for single vehicles (locomotives and wagons) and for complete freight trains becomes apparent. Therefore, a first part of the research is devoted to creating a database of geometries for vehicles and vehicle parts in formats that are compatible with software for CFD simulation. In this way, complex geometries representative of realistic freight operation scenarios can be efficiently created. In the creation of the database, a defeaturing process is applied and vehicle geometries are defined at different levels of detail, allowing the efficient creation of simpler and more detailed CFD models, in view of finding a trade-off between accuracy and computational efficiency.

This paper presents some initial results from the research. In particular, definition of the geometry database is presented, then the results of a CFD analysis of a single freight wagon is presented, comparing the results for different levels of detail of vehicle geometry.

The paper is structured as follows: in section 2 of the paper a detailed description of the geometries and the process by which they have been created and stored in the database is provided. In section 3 an exemplary CFD analysis is presented, analysing

the mesh independence and a comparison between levels of detail. Finally, in section 4 conclusion and final remarks are drawn.

2 The database of freight train geometries

Unlike passenger trains, freight trains exhibit a wide variety of geometries both because of the diversity of the wagons that make them up and because of the many different compositions (what type of wagons they are made of, and in what order) that they can have.

The study of the aerodynamics around these vehicles therefore is only possible if an efficient and versatile method for producing diverse freight train geometries is developed. The aim of the database proposed in this work is to address this need while allowing the user to balance between higher levels of detail and computational cost.

Before the construction of the database could begin, a classification of locomotives and wagon types was necessary. While no official classification exists, freight wagons can be broadly distinguished according to these categories: Open wagons, Covered wagons, Flat wagons, Dump cars, High-capacity wagons, Special wagons, and Tank wagons. Although this way of distinguishing freight wagons has been also adopted with minor variations elsewhere in literature, these specific categories have been taken from Principe [21]. Locomotives are more homogenous in their geometry, so they have not been classified in a similar way, instead three versions meant to resemble slight variations in existing locomotives are proposed. Finally, each of the geometries are provided in different levels of detail. The classification is showcased in Figure 1.

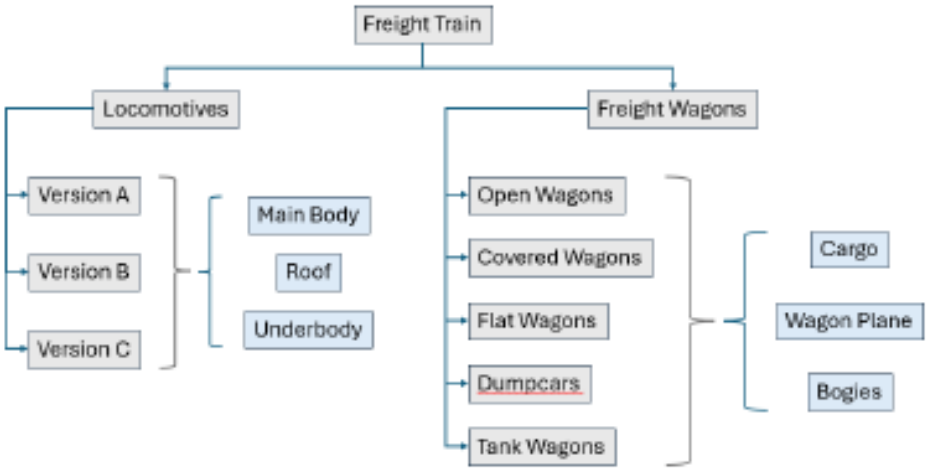

Figure 1: Classification of the database.

A modular approach is used to build the geometric models of the vehicles. All wagons are composed of three parts: a wagon plane, bogies, and cargo (where cargo refers to the geometry above the wagon plane, this is the distinguishing part of each category of wagon). In Figure 2, the components of tank wagons are shown, the cargo

of course will be different for other categories of wagon, Figure 3 shows the version B of the locomotive in its three components.

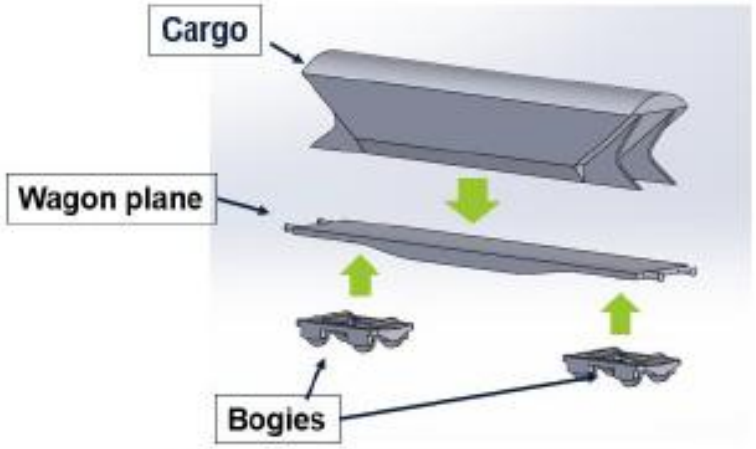

Figure 2: All wagon components.

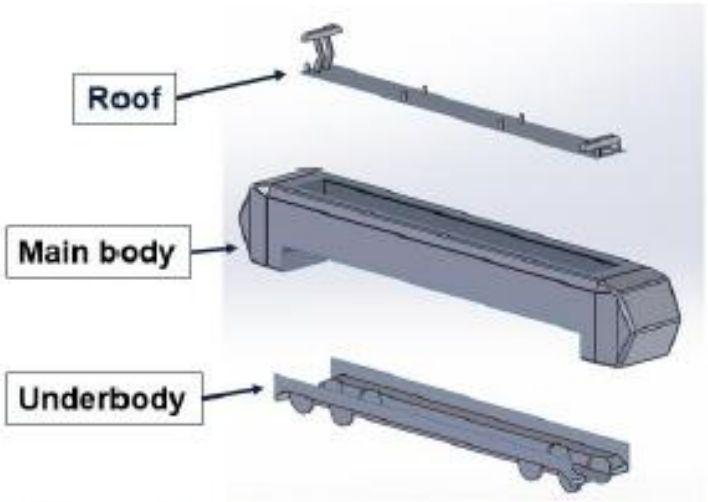

Figure 3: All components of locomotives, version B.

The database consists of the assembled geometries together with the modular parts that make them up, therefore every user will have access to the geometries of all components of the vehicles. The main advantage of structuring the database with this modular approach is that it allows the user to select the level of detail of each component and, to a degree, customize the geometry based on their necessity. Additionally, the geometries built with the same components allow to properly compare the effect of the cargo on the flow around the vehicle, while if all models were subtly different the effect of the intended and unintended differences would be confounded. As a final advantage, this approach allows for faster production and update of geometries.

The database includes geometries of both locomotives and wagons, the locomotives are made of three parts: the main body, the underbody, and the roof. What

differentiates one locomotive version from another is the main body, since the underbody and roof are designed so as to be interchangeable.

The design of the main bodies for all locomotive versions followed the same workflow: first, a basic structure is defined through the use of a certain number of parameters as shown in Figure 4, then the volume enclosed in the structure is extruded and the edges are rounded (with the radii being parametrically defined as well), and finally, the surface of the main body is obtained from the volume.

The surface obtained is at this point a closed surface, to complete the geometry it needs to be trimmed along well-defined curves. The final result is an open surface with boundaries that match those of other components of the locomotive, so that when they are all assembled, they constitute a closed surface again. Figure 5 shows the main body of the version C of the locomotive. It is worth noting that all locomotive geometries are symmetrical with respect to a plane normal to the direction of motion, therefore no additional information would be gained by reporting the entire geometry in a figure.

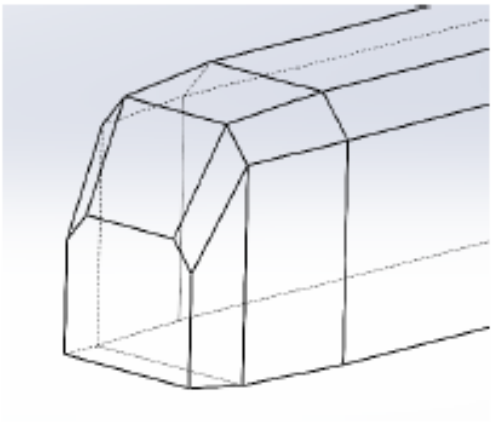

Figure 4: Structure of the locomotive, version C.

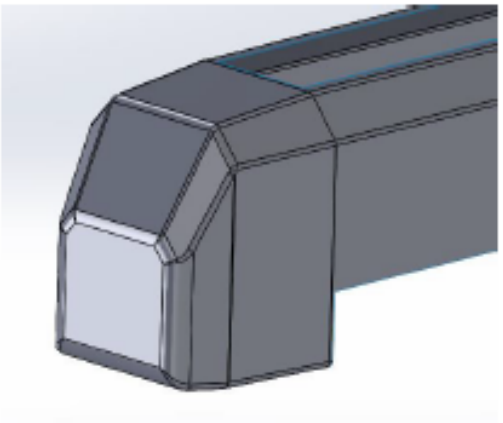

Figure 5: Main body component of the locomotive, version C.

Roof and underbody geometries in real locomotives are very different from model to model, therefore modelling a general version of these geometries is a summary endeavour by necessity, however, some parts of these geometries are standardized. In the making of the roof geometries, pantographs are surely a prominent feature, therefore they have been modelled to resemble the actual dimensions reported by Baker et al. [22]. Figure 6 shows the roof geometries, from left to right in increasing level of detail.

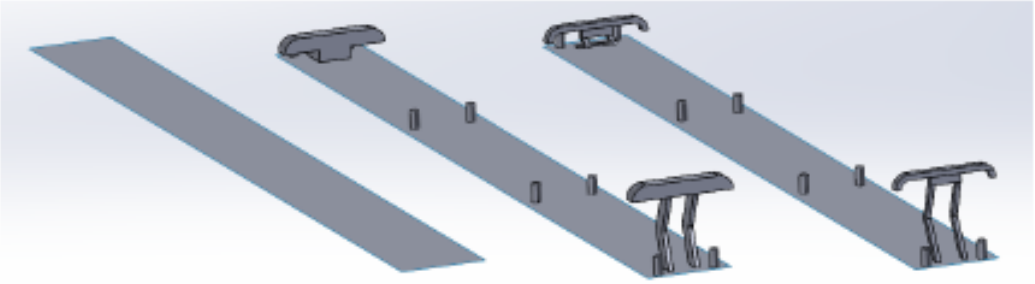

Figure 6: From left to right: Roof component, least detailed version; roof component, medium detailed version; roof component, more detailed version.

The final component of the locomotive geometry is the underbody. Similarly to the roof, the underbody geometries of actual locomotives are very diverse, and so the same strategy has been adopted; the dimensions of standardized parts have been taken from Principe [21] to make the geometry broadly realistic. Figure 7 and Figure 8 show respectively the underbody components (in increasing order of detail from left to right as before) and the complete (assembled) locomotive geometry.

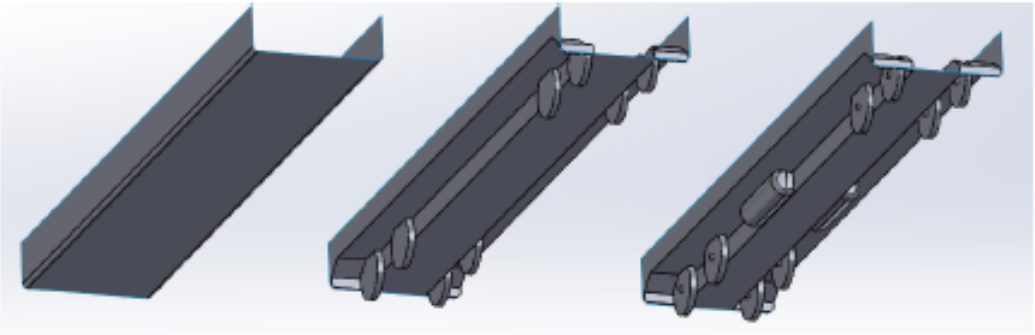

Figure 7: From left to right: Underbody component, least detailed version; underbody component, medium component version; underbody component, most detailed version.

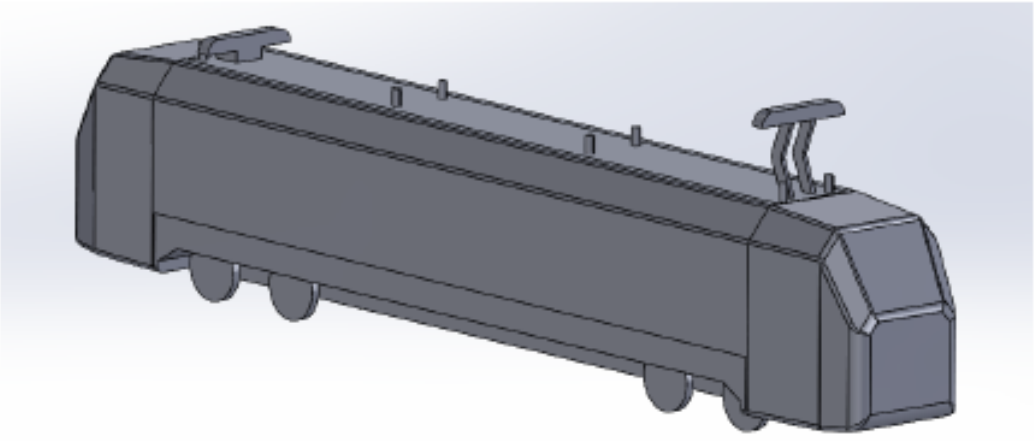

Figure 8: Assembled locomotive, version C, medium level of detail.

Like for other parts, the geometries of the roof and underbody components underwent a defeaturing process to produce the different levels of detail displayed in Figure 6 and Figure 7. The removal of details is always aimed at simplifying the mesh without sacrificing accuracy, thus the defeaturing process was carried out by removing those detail that were deemed to need a more complex profile while having little impact on the overall flow. As a general rule, features that changed the front area of the geometry were deemed more impactful on the flow than features that did not, so the former were removed only in the last iterations of defeaturing, and the latter were removed immediately. Similarly, the more voluminous features were deemed more impactful on the flow than smaller ones.

The geometry of the wagons is comprised of three components as shown in Figure 2, two of which are the same for all wagon types, for reasons already mentioned, the components referred to as bogies and plane in Figure 2 have been kept the same for all wagons, whereas the component referred to as cargo changes for the different types. However, it should be noticed that not all wagon types have a cargo, indeed flat wagons may carry one container, two container, or be empty, in the latter case the wagon is composed by plane and bogies alone.

All wagon components have been designed as closed surfaces and feature planar faces that act as interface between components. This means that all components at all levels of detail must be present planar surfaces in the right places to allow for the faces to overlap in one interface. Figure 9 shows in red the interfaces between bogies and plane and in green the one between plane and cargo.

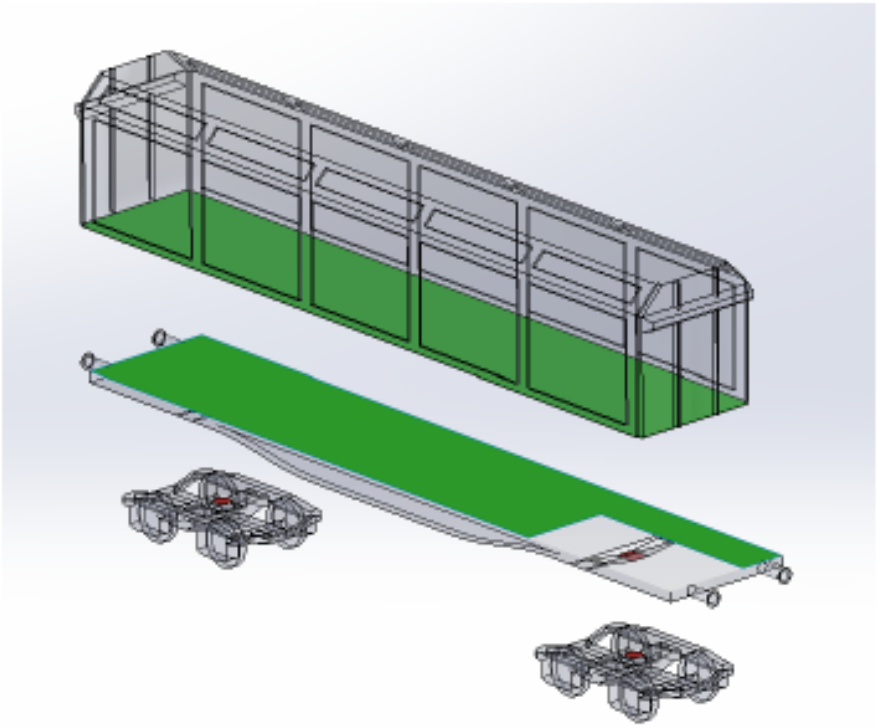

Figure 9: Components of a covered wagon with its interface surfaces highlighted.

The modelling process of the bogies was carried out using an actual 3D model of the Y25 bogies, therefore the first version of the component (see Figure 10) was the most detailed one, the less detailed versions were obtained after successive defeaturing iterations following the same criteria as outlined previously. The other components have been realized without 3D models; therefore, the opposite workflow was adopted. The simpler version was made first in such a way as to resemble the most important aerodynamic features of the commercially available models, and then more and more detailed versions were obtained as modified versions of the first one. As an example, Figure 11 shows the wagon plane in its levels of detail.
With all of the components modelled, the last step consisted in assembling and uploading the files to a public GitHub repository, available here. All the geometries have been uploaded in step format and are available both as preassembled single vehicles (the assemblies have only been made with components with consistent level of detail), and single components (available at all levels of detail).

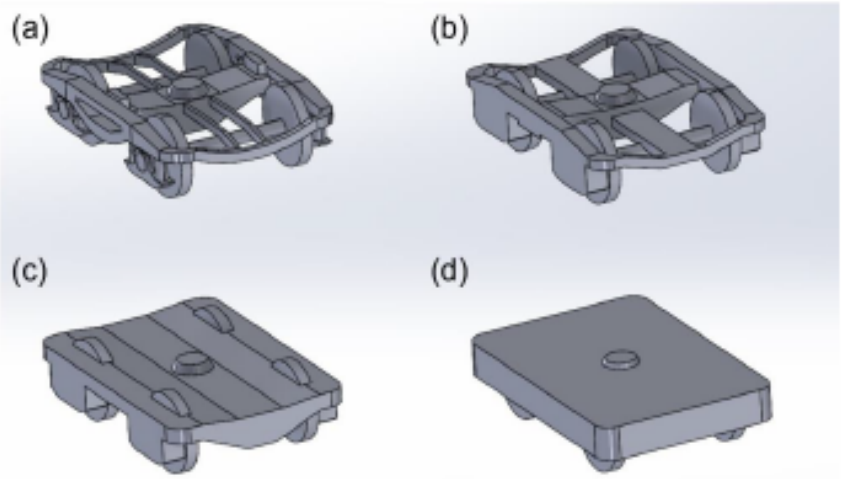

Figure 10: Bogies components in different levels of detail: (a) Most detailed; (b) More detailed; (c) Medium detailed; (d) Less detailed.

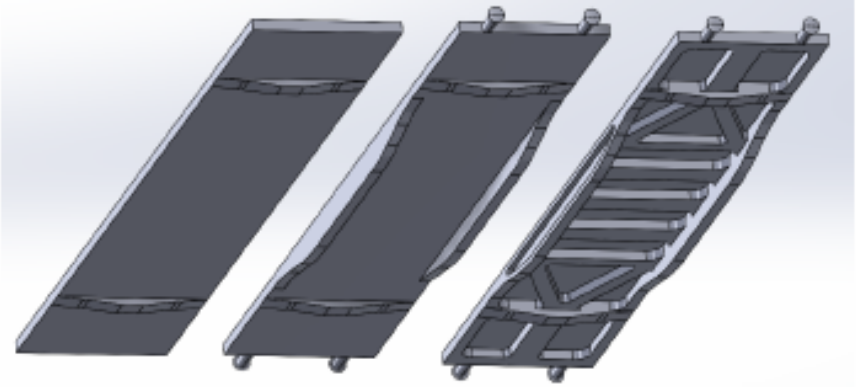

Figure 11: From left to right: wagon plane, least detailed; wagon plane, medium detailed; wagon plane, most detailed.

The database presented in this work can be used for the simulation of the aerodynamics of a generic freight train, but further improvements are possible. One possibility is the addition of more geometries, for example geometries for double stacked containers can be added to the cargo components, longer versions of some wagon types could be considered (for example, the covered wagons and the flat wagons are sometimes designed with longer planes for greater capacity), and some special purpose wagons could be added as well. Another way of improving on the present work would be to simplify the process of composing a train of chosen composition, a software to manipulate the coordinates within the files would be the most suitable tool for this.

3 CFD analysis of single wagon

In this section, the simple case of a single flat wagon with a 40 ft container moving at 160 kmh^{-1} in steady air is considered.
The simulations have been carried out using the open-source software OpenFoam v10, the solution was achieved in two steps: the first consisted in the evaluation of the steady state flow, and the second one in the calculation of the unsteady flow using the steady solution as a starting point for the simulation. The steady state simulation was carried out with the SIMPLE algorithm starting from the solution of the potential flow, the linear scheme was used for the gradient of velocity and the upwind scheme for its divergence. The k-ω SST turbulence model was adopted for both steady-state and transient runs. The unsteady simulations were carried out with the PIMPLE algorithm, using the solution from the steady one as initial conditions with the same settings as before (except of course for the time-derivative, for which the implicit Euler scheme was chosen).

Figure 12 shows the domain dimensions in terms of lengths (L), widths (W) and heights (H) of the wagon, a zero-gradient boundary condition was chosen for pressure for the ground and wagon patches, with no-slip condition for the velocity. The inlet velocity was set to 160 kmh^{-1} and at the outlet pressure a zero-gradient was imposed, zero-gradient for pressure and slip condition for velocity were set on all remaining patches.

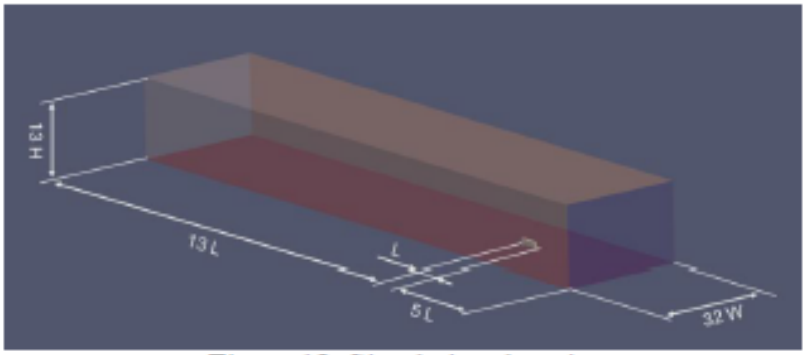

Figure 12: Simulation domain.

The meshes were all structured and have been obtained with the inbuilt OpenFoam application snappyHexMesh, with a refined region around the wagon.

For the simulations of the flow around the proposed geometries to be useful, they have at least to be independent of the grid, thus a convergence study was carried out. Table 1 reports the aerodynamic coefficients for lift and drag determined with meshes of different level of refinement in a steady-state simulations. The coefficients have been calculated using a reference area of 10 m^2 according to expressions (1).

$$C_D = \frac{2D}{\rho A {U_f}^2} \qquad C_L = \frac{2L}{\rho A {U_f}^2} \qquad C_S = \frac{2S}{\rho A {U_f}^2} \tag{1}$$

Where D is the pressure drag, L is the pressure lift, S is the pressure side force, ρ is the density of the air, A is the reference area and U_f is the freestream velocity of the air (44.44 ms^{-1})

Table 1 shows that the variations of aerodynamic coefficients remain below 1% beyond the 11.9 million cells grid, thus the results are deemed to be mesh independent beyond this level of refinement. It should be noted that, although the results remain consistent, they are numerically different from other findings in literature (Östh et al. [23]). This can be explained by the fact that the flow around freight wagons is strongly unsteady, therefore the steady-state solver should not be expected to accurately predict the value of the aerodynamic forces. This is a well know limitation of the RANS method that has been reported in the literature before by Maleki et al. [20], this method remains capable of predicting trends in aerodynamic forces and is useful for comparative investigations.

Number of cells [millions]	C_D [-]	C_L [-]	$\Delta C_D/C_D$ [%]	$\Delta C_L/C_L$ [%]
2.9	0.809	-0.207	+0.24%	-6.94%
4.4	0.811	-0.192	+0.44%	+5.84%
6.3	0.814	-0.204	+0.65%	+8.04%
8.9	0.819	-0.220	-0.06%	+1.08%
11.9	0.819	-0.222	-0.53%	-0.63%
15.6	0.815	-0.221	+0.59%	-0.44%
20.1	0.819	-0.220		

Table 1: Convergence of aerodynamic coefficients for with different grids

The URANS method, although unsteady, has been reported to be unsuitable to evaluate accurately the aerodynamic forces on a vehicle as if fails to correctly predict the length of recirculation regions (Wang et al. [18] and Maleki et al. [20]), but despite this limitation, the unsteady simulations run in this work have produced a significant improvement in the accuracy of the aerodynamic coefficients. Table 2 shows the results for force coefficients averaged over the last 5 seconds of the run for the less-detailed version and medium-detailed version of the wagon as defined in expression (1). The drag coefficients are comparable to those obtained with LES by Östh et al. [23], while the lift remains overpredicted. Finally, Figure 13 shows the magnitude velocity field on the xz-plane and Figure 14 shows the longitudinal velocity profiles on top of the container in correspondence to the white lines indicated in Figure 13, which demonstrate that the simulation captured the recirculation of the flow.

	C_D [-]	C_L [-]	C_S [-]
Less detailed wagon	0.862	-0.218	0.011
Medium detailed wagon	0.878	-0.170	0.006

Table 2: Time-averaged aerodynamic coefficients from unsteady simulations.

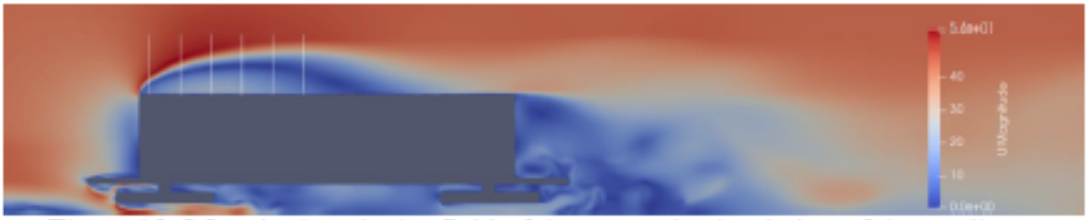

Figure 13: Magnitude velocity field of the unsteady simulation of the medium detailed geometry.

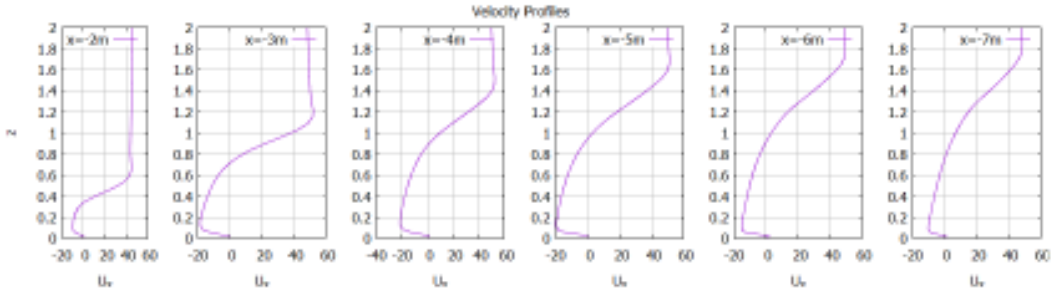

Figure 14: Profiles of the x component of the velocity on top of the container.

4 Conclusions and Contributions

In this work, a database for the efficient production of surface geometries for the CFD simulations of freight trains has been proposed, and some demonstrational steady and transient simulations have been run on the geometry of a container wagon at a lesser and higher level of detail. The database allows for the user to choose between different types of wagons, and to compose the wagon with individual components. In this way the user can form a single wagon or an entire train with components having different levels of detail in different parts, allowing for the efficient production of customized freight trains geometries.

With proper grids, the steady simulations reached consistent results for aerodynamic force coefficients but failed to replicate the more accurate results obtained in literature with methods better suited for unsteady flows; in particular, they underpredicted the drag and overpredicted the lift. The failure of the RANS method to accurately evaluate aerodynamic forces on the vehicle is explained by its inability to capture the markedly unsteady nature of the flow, with the result of obtaining a non-physical solution. A significant improvement was provided by the URANS simulations which managed to reproduce results for the drag well comparable with more accurate methods (discrepancies with LES within 5%), although with overprediction of the lift. Additionally, the unsteady method managed to capture the recirculation region on top of the container near the leading edge.

Acknowledgements

The research reported in this paper has received funding from the European Union's Horizon Europe research and innovation programme under grant agreement: HORIZON-ER-JU-2022-ExplR-04. Views and opinions expressed are however those of the authors only and do not necessarily reflect those of the European Union or Europe's Rail Joint Undertaking. Neither the European Union nor the granting authority can be held responsible for them.

References

[1] J. Geischberger and M. Moensters, "Impact of faster freight trains on railway capacity and operational quality," *International Journal of Transport Development and Integration*, vol. 4, no. 3, pp. 274–285, Jul. 2020, doi: 10.2495/TDI-V4-N3-274-285.

[2] A. Quazi, T. Crouch, J. Bell, T. McGreevy, M. C. Thompson, and D. Burton, "A field study on the aerodynamics of freight trains with different stacking configurations," *Journal of Wind Engineering and Industrial Aerodynamics*, vol. 232, Jan. 2023, doi: 10.1016/j.jweia.2022.105245.

[3] F. Alam and S. Watkins, "Lateral stability of a double stacked container wagon under crosswind," *Proceedings of the International Conference on Mechanical Engineering 2007*, 2007.

[4] S. Maleki, D. Burton, and M. C. Thompson, "Flow structure between freight train containers with implications for aerodynamic drag," *Journal of Wind Engineering and Industrial Aerodynamics*, vol. 188, pp. 194–206, May 2019, doi: 10.1016/j.jweia.2019.02.007.

[5] D. Flynn, H. Hemida, D. Soper, and C. Baker, "Detached-eddy simulation of the slipstream of an operational freight train," *Journal of Wind Engineering and Industrial Aerodynamics*, vol. 132, pp. 1–12, 2014, doi: 10.1016/j.jweia.2014.06.016.

[6] C. Li, D. Burton, M. Kost, J. Sheridan, and M. C. Thompson, "Flow topology of a container train wagon subjected to varying local loading configurations," *Journal of Wind Engineering and Industrial Aerodynamics*, vol. 169, pp. 12–29, Oct. 2017, doi: 10.1016/j.jweia.2017.06.011.

[7] D. Flynn, H. Hemida, and C. Baker, "On the effect of crosswinds on the slipstream of a freight train and associated effects," *Journal of Wind Engineering and Industrial Aerodynamics*, vol. 156, pp. 14–28, Sep. 2016, doi: 10.1016/j.jweia.2016.07.001.

[8] F. Alam and S. Watkins, "Effects of Crosswinds on Double Stacked Container Wagons," Gold Coast, Australia, Dec. 2007.

[9] S. Giappino, D. Rocchi, P. Schito, and G. Tomasini, "Cross wind and rollover risk on lightweight railway vehicles," *Journal of Wind Engineering and Industrial Aerodynamics*, vol. 153, pp. 106–112, Jun. 2016, doi: 10.1016/j.jweia.2016.03.013.

[10] A. Kocoń and A. Flaga, "Critical velocity measurements of freight railway vehicles roll-over in wind tunnel tests as the method to assess their safety at

strong cross winds," in *Journal of Wind Engineering and Industrial Aerodynamics*, Elsevier B.V., Apr. 2021. doi: 10.1016/j.jweia.2021.104559.

[11] D. Soper, C. Baker, and M. Sterling, "Experimental investigation of the slipstream development around a container freight train using a moving model facility," *Journal of Wind Engineering and Industrial Aerodynamics*, vol. 135, pp. 105–117, Dec. 2014, doi: 10.1016/j.jweia.2014.10.001.

[12] M. Sterling, C. J. Baker, S. C. Jordan, and T. Johnson, "A study of the slipstreams of high-speed passenger trains and freight trains," *Proc Inst Mech Eng F J Rail Rapid Transit*, vol. 222, no. 2, pp. 177–193, 2008, doi: 10.1243/09544097JRRT133.

[13] S. Giappino, S. Melzi, and G. Tomasini, "High-speed freight trains for intermodal transportation: Wind tunnel study on the aerodynamic coefficients of container wagons," *Journal of Wind Engineering and Industrial Aerodynamics*, vol. 175, pp. 111–119, Apr. 2018, doi: 10.1016/j.jweia.2018.01.047.

[14] D. Soper, C. Baker, and M. Sterling, "An experimental investigation to assess the influence of container loading configuration on the effects of a crosswind on a container freight train," *Journal of Wind Engineering and Industrial Aerodynamics*, vol. 145, pp. 304–317, 2015, doi: 10.1016/j.jweia.2015.03.002.

[15] M. Bocciolone, F. Cheli, R. Corradi, S. Muggiasca, and G. Tomasini, "Crosswind action on rail vehicles: Wind tunnel experimental analyses," *Journal of Wind Engineering and Industrial Aerodynamics*, vol. 96, no. 5, pp. 584–610, May 2008, doi: 10.1016/j.jweia.2008.02.030.

[16] D. Soper and C. Baker, "A full-scale experimental investigation of passenger and freight train aerodynamics," *Proc Inst Mech Eng F J Rail Rapid Transit*, vol. 234, no. 5, pp. 482–497, May 2020, doi: 10.1177/0954409719844431.

[17] D. Soper *et al.*, "Full scale measurements of train underbody flows and track forces," *Journal of Wind Engineering and Industrial Aerodynamics*, vol. 169, pp. 251–264, Oct. 2017, doi: 10.1016/j.jweia.2017.07.023.

[18] S. Wang, J. R. Bell, D. Burton, A. H. Herbst, J. Sheridan, and M. C. Thompson, "The performance of different turbulence models (URANS, SAS and DES) for predicting high-speed train slipstream," *Journal of Wind Engineering and Industrial Aerodynamics*, vol. 165, pp. 46–57, Jun. 2017, doi: 10.1016/j.jweia.2017.03.001.

[19] S. Wang, J. R. Bell, D. Burton, A. H. Herbst, J. Sheridan, and M. C. Thompson, "The performance of different turbulence models (URANS, SAS and DES) for predicting high-speed train slipstream," *Journal of Wind Engineering and Industrial Aerodynamics*, vol. 165, pp. 46–53, 2017.

[20] S. Maleki, D. Burton, and M. C. Thompson, "Assessment of various turbulence models (ELES, SAS, URANS and RANS) for predicting the aerodynamics of freight train container wagons," *Journal of Wind Engineering and Industrial Aerodynamics*, vol. 170, pp. 68–80, Nov. 2017, doi: 10.1016/j.jweia.2017.07.008.

[21] E. Principe, *Il Veicolo Ferroviario*. Roma: Collegio Ingegneri Ferroviari Italiani, 2010.

[22] C. Baker *et al.*, *Train Aerodynamics: Fundamentals and Applications*. Cambridge: Butterworth-Heinemann, 2019.

[23] J. Östh and S. Krajnović, "A study of the aerodynamics of a generic container freight wagon using Large-Eddy Simulation," *J Fluids Struct*, vol. 44, pp. 31–51, Jan. 2014, doi: 10.1016/j.jfluidstructs.2013.09.017.

Appendix B: paper “A review of freight trains aerodynamics”

This paper was submitted to the Proceedings of the Institution of Mechanical Engineers, Part F: Journal of Rail and Rapid Transit and is presently under second review.

In the following pages, the revised manuscript submitted for the second review is reported in the same format as submitted to the journal, i.e. with text in red colour representing additions with respect to the originally submitted manuscript and with text in red colour + strikethrough representing deletions with respect to the initially submitted manuscript.

A review of freight trains aerodynamics

Luca Corniani[a]*, Paolo Schito[a], James Bell[b], Stefano Bruni[a]

[a]*Dipartimento di Meccanica, Politecnico di Milano, Milano, Italy;*

[b]*Institute of Aerodynamics and Flow Technology, German Aerospace Center (DLR), Göttingen, Germany;*

*corresponding author: Luca Corniani, luca.corniani@polimi.it, Dipartimento di Meccanica, Politecnico di Milano, Via La Masa 1, 20156, Milano, Italy

Abstract. Research on train aerodynamics has so far mostly focused on high-speed passenger trains. However, increasing evidence is being acquired showing that aerodynamic effects are also highly relevant to freight trains regarding their efficient and safe operation. Freight-train-specific aerodynamic phenomena become more relevant in light of the increase ~~of~~ in freight train service speed expected to take place in the near future.

For some decades now, experimental and numerical studies have been published about the aerodynamics of freight trains, and specifically of container trains. An overview of this effort is presented in this paper, the major points of agreement are summarized, and the open points in the field are identified.

In the paper, the topology of the flow and the slipstream are described and their implications on the aerodynamic forces (both with and without crosswinds) are discussed. Special attention is given to aerodynamic resistance, drag and to the efforts made in literature to predict it using numerical and experimental methods. Furthermore, a comparison of the methods of investigation adopted in the field is presented, highlighting their suitability for the study of different problems. Finally, other topics like the risk for bystanders caused by slipstream effects, ballast flight and aerodynamics in tunnels are discussed.

The literature review highlights the need to expand the research on freight train aerodynamics to freight train geometries different from intermodal container trains and to consider the many diverse geometries that may result from realistic mixed compositions of different wagon types.

~~This review is meant to provide an overview of the knowledge acquired up to now about the flow around freight trains and the aerodynamic forces acting on the wagon, identify good~~

~~practices emerging from the literature and outline some potential future developments of research in the field.~~

Keywords: Train aerodynamics, Freight trains, Drag, Crosswinds, slipstreams, TSI

1. Introduction

The declared goal of the European Union (EU) for the transportation sector is to reduce greenhouse gas emissions by 20% with respect to their 2008 level by 2030, and ~~of reducing~~ to reduce them by 60% with respect to 1990 by 2050 (1). In light of these goals, several actions are foreseen by the EU, including the shift of freight transportation from other modes to ~~the~~ rail. More specifically, it is envisaged that at least 30% of road-transported freight should be shifted to rail or waterways by 2030, and at least 50% should be shifted by 2050 (1). Increasing the share of freight transported on rail is indeed an effective measure for reducing CO_2 emissions, given that trains emit 16 g/tkm, compared to the 118 g/tkm emitted by heavy road vehicles and the 33 g/tkm emitted by freight transportation performed on inland waterways (2).

~~In this context, improving freight train aerodynamics is pivotal towards reducing drag resistance, which is the most effective means to improve the energy efficiency of this transport mode, thereby improving its profitability and further reducing its ecological footprint.~~ In this context, reducing drag resistance provides further substantial improvement. ~~At current freight train service speeds, aerodynamic drag already takes a large share of the overall resistance to forward motion: at~~ At just 115 km/h, the contribution of aerodynamic drag to overall resistance to motion can be as much as 80% of the total ~~(Li et al.~~ (3)~~)~~. Furthermore, it should be considered that the service speed of freight transportation on rails is expected to grow significantly in the near future, at least for some specific freight types, targeting a service speed of 160 km/h and beyond ~~(Boehm et al.~~ (4)~~)~~. Given that aerodynamic forces grow approximately with the square of the speed, any increase in the service speed of freight trains means that the share of aerodynamic effects in the overall resistance to forward

motion will become even more important. ~~Therefore, improving freight train aerodynamics is pivotal towards increasing the competitiveness of rail freight transport, without undermining the ecological benefits that make this mode desirable in the first place~~.

~~It should be noted that~~ Furthermore, reducing drag resistance is not the only open issue in freight train aerodynamics, and other factors need to be addressed, namely the effect of crosswinds and slipstream effects, i.e. the effects caused by the air dragged along by the freight train while it runs on the railway track (5,6)~~. As a train moves in the air, it drags air along with it, and the air set in motion by the train is called the slipstream. Faster and bulkier trains produce stronger slipstreams on platforms that may be dangerous to passengers on platforms and railway workers~~ While slipstream effects have been in the past mostly investigated for passenger trains, there is a need to achieve a better understanding of these effects for freight trains, considering their complex geometry and large shape variability. Furthermore, the non-aerodynamic, bluff shapes of freight trains perturb air flow in tunnels, ~~hindering the flow of air outside the tunnel and~~ increasing the pressure build-up ahead of the train , thus increasing drag resistance and leading to dynamic over-pressure which may affect the tunnel's structural resistance and generate additional forces on a crossing train (7). ~~Finally, the bluff shapes of freight trains may cause strong underbody air flows, thus facilitating ballast flight and causing it to occur at lower speeds compared to passenger trains.~~ Finally, freight trains often have heavier axle loads (8) and more bluff shapes than passenger trains: these two concomitant features can cause increased mechanical forces on the tracks and stronger airflows in the underbody, thus facilitating ballast flight at lower speeds than passenger trains (9).

~~Therefore~~ In summary, ~~fast~~ high-speed freight trains face ~~many~~ numerous aerodynamic challenges that hinder their wide adoption and, ~~while some of these challenges are the same faced by~~ compared to high-speed passenger trains, the bluff shape of the wagons produces more complex airflow patterns ~~that might lead to issues~~ with effects that have been so far seldom analyzed. Freight

trains are also characterized by large shape variability, featuring very diverse geometries for locomotives and wagons, and are operated under highly variable operating conditions which include different mixes of wagon types, variable inter-car gaps and the use of double-stacked containers (8).

The above considerations highlight the present and growing importance of aerodynamic effects in freight train vehicles. The complexity and variety of the phenomena have spurred researchers to study all the aspects of the flow, ~~thus~~ and therefore a review that collects and compares the various approaches and results of this effort is ~~necessary~~ useful and timely. This ~~paper~~ work aims to perform a thorough analysis of the existing state-of-the-art in this emerging field as the starting point for ongoing and future research.

The paper is organized as follows: Section 2 provides a historical perspective on how the topic has been treated in scientific literature. In Section 3 an overview of the current problems and methodologies will be given. Then, in Section 4 the topics most frequently addressed in scientific literature will be discussed in greater detail. Finally, in Section 5 some considerations on the possible future developments of the field will be presented.

2. Historical summary

Different methods have been used over the past decades to investigate the aerodynamics of freight trains, both because of the progress in research methods and the increase in computational power. In this section a historical summary is given of the research effort in this field, highlighting the increased interest attracted by this topic in recent years and summarizing the research methods ~~deployed~~ applied and the specific sub-topics investigated. The summary considers a total of 80 ~~66~~ research papers, i.e. references (3-7), (9,10), (20-89), and (92,93). ~~(3,10) and (14-76).~~

Figure 1 analyses the amount of research work done on the subject in past years, based on the number of papers published in different 5-year periods, also showing for each time period the share

of papers characterized by analytical vs. experimental approaches to the subject. Note that the papers making use of both numerical and experimental methods have been counted in both groups.

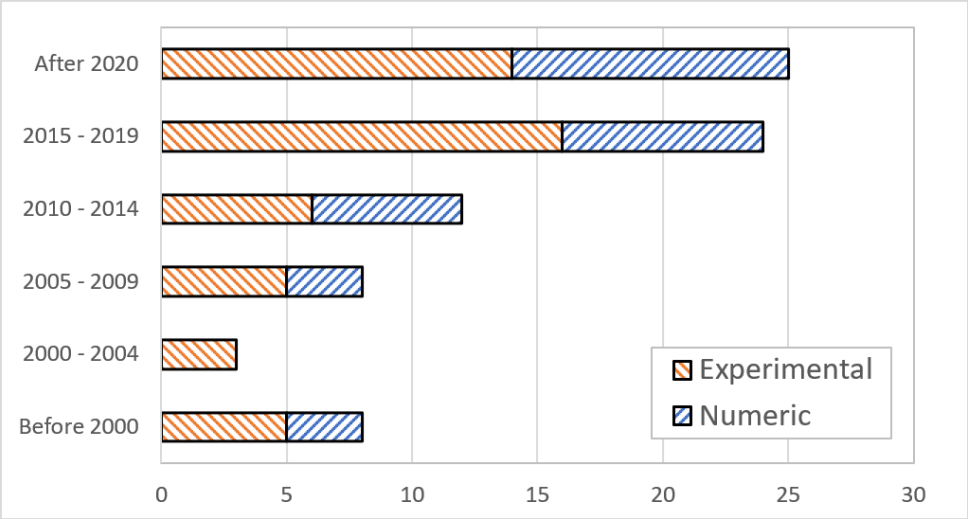

Figure 1, Papers published on freight-train aerodynamics sorted by numerical or experimental and by year of publication.

~~The partition between experimental and numerical works is far from perfect, but it is still useful for highlighting some aspects of the research conducted so far in the field.~~ The first point worth noticing is the significant increase in interest raised ~~by the~~ in this topic in recent years, with most publications cited in this work having appeared in the last 10 years. Another point worth noticing is that the proportion between numerical and experimental works has not changed dramatically over the years, with the experimental methods being slightly more frequent than numerical ones. This is despite the increase in computational power in recent decades enabling the use of more complex numerical methods (10). ~~an approximately equal share of these two methodologies of investigation.~~

Figure 2 presents a classification of the references based on the research topics addressed which are: drag (which includes also some works about the overall train resistance, not only aerodynamic drag), overturning stability (which includes all the works that study the aerodynamic forces that contribute the overturning moment), flow characterization (which includes all the works

that study the flow structures generated by the wagons, the slipstream and pressure field) and other (which includes all the works that deal with problems that don't fit in any of the previous categories, like ballast flight or flow in tunnels). Some works investigate more than one theme, so they have been counted in each relevant category.

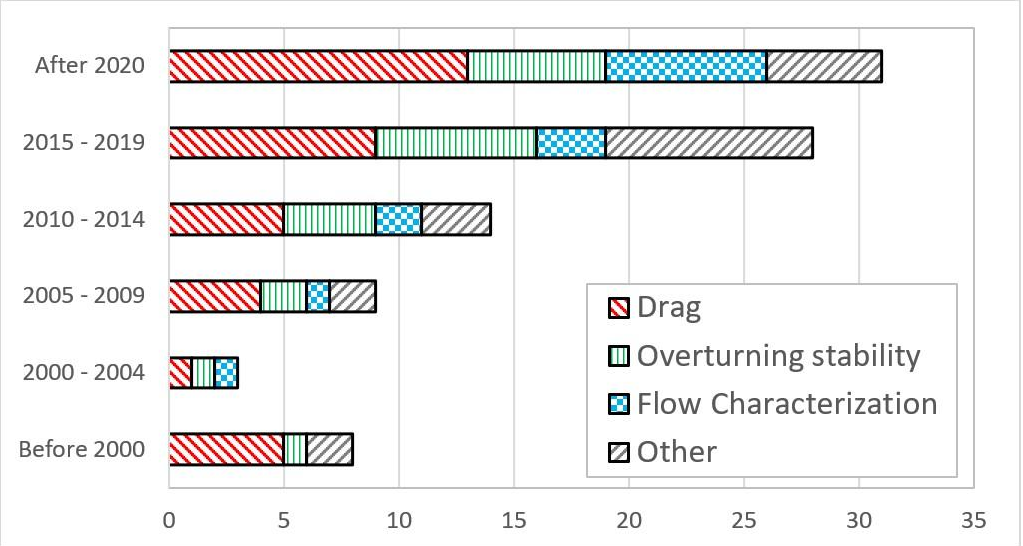

Figure 2, Papers published on freight-train aerodynamics sorted by topic of the investigation and by year of publication.

As is clearly noticeable from Figure 2, drag is the most studied "macro topic" in all the periods considered, and the proportion of the works dedicated to it is growing. This is explained by the immediate impact that aerodynamic drag has on the overall train resistance, making it the key topic to be investigated in view of economic and environmental benefits.

Some considerations on the research trends can be made based on these two figures. Firstly, it is clear that numerical methods have not replaced experimental ones: in fact, most of the works that make use of numerical methods also validate numerical results through a comparison with experimental data. This supports the view that numerical and experimental methods should be thought of as complementary, rather than the former being the substitute for the latter. Thus, it is expected that

experimental investigations will remain pivotal to the advancement of research in the field. Secondly, works related to drag, overturning stability and slipstream (with the last being grouped here with 'Flow characterization') have also become more popular in recent years. This is in response to the current (and future) need for the safe and efficient operation of freight trains in light of the expected increase in speed.

2.1 Standards and regulations

To complement the survey of the research papers provided above, a summary of standards and regulations addressing freight-train aerodynamics is outlined here, considering the EN standards and the Technical Specifications for Interoperability (TSIs). It should be noted that, in some cases, these standards and regulations are defined for passenger trains and therefore do not apply to freight trains in a strict sense but, due to the lack of specific regulations, they are often taken as a useful reference also for freight trains.

The TSIs (11) address the aerodynamic effects produced by rail vehicles in terms of slipstream, head pressure pulse, pressure variation in tunnels, crosswinds stability and ballast flight (although only national regulations apply to the aerodynamic effects on ballasted tracks, and only for rolling stock travelling at speeds of at least 250 km/h).

The relevant standard for aerodynamics in railway applications is EN 14067, consisting of 6 parts. Part 1, (EN 14067-1 (12)) is equally applicable to passenger and freight trains, as it simply defines the symbols and units for the remaining parts of the standard. A description of the flow around trains in tunnels and of the pressure waves they generate is provided in part 3 (see EN 14067-3 (13)). It applies to freight trains, stating that the effect of pressure peaks caused by pressure waves on the cargo shall be taken into account when operating open freight trains. It is also highlighted that pressure waves may cause severe discomfort to railway workers and passengers (if the train is not properly sealed) and may cause fatigue damage to some infrastructure components. This is especially true in

the worst-case scenario in which the superposition of four positive compression waves (caused by the simultaneous passage of two trains in opposite directions in the same tunnel), causes the amplitude of the total pressure to become as high as 3.5 times the amplitude of the single compression waves.

The requirements concerning aerodynamics in open tracks, and the methodologies for accessing conformity with these requirements are addressed in EN 14067-4 (14) which prescribes limitations on the peak-to-peak pressure changes (head pressure pulses) and slipstream velocities in an open field. However, these requirements only apply to trains travelling at speed above 160 km/h, hence not to currently operationg freight trains. ~~Although freight trains are not explicitly excluded by these limitations, freight trains remain unaddressed because thresholds are defined only for trains travelling at speeds above 160 km/h, see also Section 0~~. Full-scale, model-scale and CFD methodologies are discussed as a means to assess conformity to requirements. Analytical methods to calculate the dynamic loads caused by the air on flat surfaces parallel to the tracks are also provided and, since these methods are independent from train geometry, they are in principle applicable to freight trains too. Finally, methods to evaluate the overall resistance to motion are provided.

Part 5 of the standard (15) provides requirements and assessment procedures for aerodynamics in tunnels. Pressure variations caused by the passing of a train in a tunnel may cause aural discomfort or damage to passengers and rail workers, so thresholds are given for these pressure changes. However, similarly to part 4, freight trains are in practice unaddressed as no thresholds are indicated for trains operating under 200 km/h. The norm also describes methodologies to evaluate the pressure gradient of the compression wave (only for vehicles faster than 200 km/h) and resistance to aerodynamic loads (meaning loads given by the pressure difference between inside and outside the vehicle). Freight wagons are explicitly excluded by this latter requirement, but freight locomotives are subject to it for speeds above 140 km/h.

Finally, requirements and test procedures for crosswind assessment are outlined in EN 14067-6 (16). It applies to freight trains travelling at 80 km/h speed or higher (while national requirements exist in some EU countries at even lower speeds). The characteristic wind speeds are defined as the maximum wind speed allowable before the rolling stock reaches a lower threshold of the wheel unloading coefficient, leading to the risk of overturning. When these values are listed for varying input parameters (such as train speed or yaw angle), these curves are characteristic wind curves (CWC). The current requirements for CWC of freight trains are set by individual countries. For the determination of the relevant aerodynamic coefficients (typically the moment coefficient of the overturning moment, see Section 0), both CFD and wind-tunnel experiments can be used. Finally, a cursory treatment of infrastructure response to crosswinds is indicated, but it is only applicable to passenger trains.

This overview of regulations regarding rail vehicle aerodynamics shows that a quite large part of the existing standards leaves freight trains mostly unaddressed. This is either because they are explicitly excluded from the scope of the prescriptions, or because the lower speed boundary for applicability is beyond the range of freight trains' speeds. ~~Although~~ Despite the lack of specific regulations, the aerodynamic effects produced by freight trains are often comparable or even more severe than those produced by passenger trains at higher speeds (see for example Section 0).

3. Topics and methods in freight-train aerodynamics

In this section, a summary of the aerodynamic issues that arise with modern and future freight trains is presented, as well as the methods employed to study them.

~~The geometry of freight wagons poses a two-fold challenge to aerodynamic investigation, which is specific to freight train aerodynamics. Firstly, the strongly unsteady flow that is generated by wagon geometry requires, especially for numerical studies, the use of methods and tools able to capture and account for transient phenomena. Secondly, freight wagons have very different~~

~~geometries from one another, thus making it more difficult to generalize the results obtained while considering one single specific geometry.~~

The geometry of freight wagons poses challenges to aerodynamic investigation, which are specific to freight-trains. Freight wagons have bluff geometries with sharp corners; this causes the flow to be more turbulent and more strongly unsteady because of flow separation. To overcome this challenge, numerical and experimental studies need to employ methods that can capture the transient phenomena of the flow. Furthermore, freight wagons have very different geometries from one another, and therefore the results obtained for one train composition are very difficult to generalize to other geometries. This diversity of shapes also has a very large impact on standardization approaches, and on how to appropriately define a freight train.

In past research, the diverse geometries of freight trains have seldom been considered. Instead, significant efforts have been made to study the aerodynamics of intermodal container trains, almost to the exclusion of other wagon geometries. The focus on this type of wagon is in part justified by the growing intermodal share in European rail freight transport in the last decades (17,18) ~~(see references the report by the International Union of Railways (17) and (18))~~.

3.1 Research topics in freight-train aerodynamics

Remarkable attention has been given to the study of aerodynamic drag, which is a key factor for high-speed freight trains, considering that aerodynamic forces grow approximately with the square of the velocity ~~(Davis~~ (19)~~)~~ and can account for up to 80% of the overall resistance to motion even at relatively low speeds ~~(see Li et al.~~ (3)~~)~~.

Numerical and experimental methods have been employed to investigate both drag and lift forces acting on freight wagons. Experimental methods are those that aim to acquire data about the flow around trains by making measurements on full-scale or model-scale physical airflows, numerical methods are those methods that aim to predict characteristics of the flow by calculating them (these

include computational fluid dynamics (CFD) simulations, but also numerical algorithms and experimental formulas to predict aerodynamic forces).

~~Particular attention was devoted to the aerodynamic drag of intermodal freight trains since they are the fastest-growing sector of rail freight transport in Europe (18) and the prescription to improve the aerodynamic performance of these trains would be relatively easy to implement.~~ Numerous studies have predicted the drag of these trains in open air using a numerical approach (20–23) ~~(Maleki et al. (20), Maleki et al. (21), Östh and Krajnović (22) and Garcia et al. (23))~~, wind-tunnel experiments (3,24,25) ~~(Li et al. (3), Giappino et al. (24), Siegel et al. (25))~~ and full-scale measurements (26,27) ~~(Quazi et al. (26)~~(1)~~, Quazi et al. (27))~~. Generally, good agreement between CFD and model-scale experiments has been found in the prediction of aerodynamic forces. Significant discrepancies exist between these results and full-scale experiments (see Section 0).

~~In the presence of crosswinds, the train is also subject to another aerodynamic force component, i.e., the side force and to the overturning moment (defined as the rolling moment about the point of contact between the rail and the wheel on the leeward side of the vehicle, see Figure 7). Together with the lift, the side force is of interest mainly for the safe operation of the train, as the combined effect of these two force components can lead to derailment and overturning if not properly managed.~~ ~~Hemida and Baker~~ The effect of crosswinds on the safety against overturning of freight trains was investigated numerically using the Large Eddy Simulation (LES) method ~~(28) investigated the effect of these forces on the safety against overturning of freight trains using a Large Eddy Simulation (LES) method~~, but this subject has been mostly studied experimentally by means of wind-tunnel tests (24,29–32) ~~(Golovanevskiy et al. (29), Alam and Watkins (30), Kocoń and Flaga (31) Giappino et al. (24) and Soper et al. (32))~~. Some studies have also investigated the aerodynamic drag of freight trains in tunnels~~: examples of~~ with numerical (33) and experimental (34) methods. ~~investigations of this topic are found in Iliadis et al. (33) and Iliadis et al. (34) respectively.~~

Safe operation of freight trains is not only concerned with the risk of overturning but also with slipstream effects (see Section 0 for a more in-depth discussion), to reduce the risk to passengers standing on the platforms and to maintenance workers. Measurements were gathered during full-scale experimental campaigns (35) ~~by Bell et al. (35)~~ to characterize the slipstream velocities around intermodal container trains and ~~while Flynn et al. (5) and Flynn et al. (36) used~~ Delayed Detached Eddy Simulation (DDES) were used in (5,36) to evaluate the slipstream velocities in crosswind conditions and estimate the probability of person instability i.e. the occurrence of a slipstream so intense that it can destabilize people standing in the wake of the train.

Several works have attempted to characterize the flow structures of intermodal container trains using both experimental and numerical methods, with a significant share of this effort being aimed at studying the effect of the size of the gaps between containers (3,21,22,25,27,37,38) ~~(Östh and Krajnović (22) , Li et al. (3), Quazi et al. (27), Maleki et al. (21), Soper et al. (39), Buhr et al.(38), Siegel et al. (25)).~~

		Experimental			Numerical			Elaborations of data from previous works		
		Full- scale	**Moving model**	**Wind tunnel**	**RANS, URANS**	**LES, ELES, DES, DDES…**	**Other**	**Data from CFD**	**Data from CFD and Exp.**	**Data from Exp.**
Drag	**General**	(19,26, 27,40)	(37)	(20,23,33 ,41,42)	(20,23, 33,41,4 3)	(20–22,41,44)	(45,46)		(38)	(47,4 8)
	Overall resistance	(40,49, 50)		(51)			(46,52)			(47,4 8)
	Effects of crosswinds	(26,27, 29)		(24,29)		(44,51)	(44,52)		(38)	
	Effects of gap size	(26,27)		(3,24,25)	(53)	(21,22,51)	(46,52)		(38)	(47)
	Proposed equations	(26–28)		(3)		(45)	(52)		(38)	(47)
	Novel methods	(26,49)		(43)	(54)	(55)	(52,56, 57)			(47)
	Flow in tunnels		(34)		(33,58)		(59–61)			

Lateral Forces	**General**	(26,62)	(32,37, 63)	(24,29–31,52,64–66)	(67,68)	(28,51,66,69)				(70,71)
	Effects of gap size		(32)	(24,31)		(51)				
	Effect of moving ground		(65,72)	(65)	(28,67)					
	Proposed equations									
	Novel methods		(72)	(31)	(54)		(56,57)			
Flow-field	**General**		(73)	(74)	(41,67)	(41)				(70)
	In crosswinds	(35,75)	(65)	(65,66)		(5,28,51, 66)				
	Slipstream	(35,76, 77)	(39,73, 78,79)	(74,80)	(20,41)	(5,20,36, 41)			(6,76,81,82)	
	Effects of gap size	(35)	(7,79)	(25)	(20)	(20–22,51)				
	Person instability	(76)	(39,78)			(5,36)			(76)	(70)
	Flow structures	(26,27, 35,76)	(32)	(25,74)	(20,23, 33,41)	(20–22,28,41, 51)				
	Surface pressure fields		(65)	(3,7,25,65)	(20,23, 67)	(5,20–22,28,69)				
	Proposed laws	(35)								
	Novel methods	(75)	(73)		(54)	(56,57)				
	Freight vs passenger trains	(77)							(6,76)	
Other	**General**		(37)	(83)			(45)			(9,48 ,84)
	Embankment geometry		(78)	(66)	(66)					
	Vehicle intersection				(85)	(69)				
	Ballast flight	(86)	(87)	(83)		(87,88)				(9)
	Proposed laws						(45)			
	Novel methods	(77)			(54,89)	(56,57,88)				
	Pressure waves		(34)							

Table 2, Summary of topics investigated, and methods used in freight-train aerodynamics.

3.2 Methods of Investigation

In Table 2 the papers examined in this work are sorted by the topic addressed, see the rows of the table, and by the methodology followed in the study, see the columns. In particular, in terms of the

methods, a distinction is made between “experimental”, ”numerical” and “Elaboration of data from previous works”. This last column contains works that do not provide new measurements but review and elaborate on data from different past works to highlight certain aspects. One such example is a ~~the~~ work ~~by Sterling et al.~~ in which the authors analyzed data from previous full-scale and model-scale experimental measurements to discuss and compare the slipstream of high-speed passenger trains and freight trainset (6). The three main methodologies are further divided as shown in the header of the columns. The table provides an overview of the relationships between the topics investigated and the methods of investigation most frequently used. It should be noted that some references appear in multiple cells of the table, as they address multiple research topics and/or employ more than one investigation method.

3.2.1 Experimental methods

Experimental methods can be further subdivided into full-scale experiments, wind-tunnel experiments and moving-model experiments. Moving-model experiments are methods in which a scaled model of the train is propelled along a rail rig. Some often-cited examples are the Transient Aerodynamic Investigation (TRAIN) rig in Birmingham and the moving-model facility at DLR, Göttingen.

Full-scale tests are considered the most realistic method of investigation because (unlike numerical methods) they are not subject to errors in the formulation of the physical model and (unlike scaled-model experiments) are not subject to errors due to scaling effects, differences in the Reynolds number, and differences in geometry from the actual rolling stock. The Reynolds number (Re) is a dimensionless quantity that measures the proportion of viscous and inertial forces in a flow. It is used to ensure similarity between flows at different scales and is defined as in Eq. 1.

$$Re = \frac{L_{ref} U_{ref}}{\nu} \tag{1}$$

Where L_{ref} is the characteristic length of the flow, U_{ref} is the characteristic velocity of the flow and v is the kinematic viscosity of the fluid.

On the other hand, full-scale experiments are more expensive and time-consuming than experiments on scaled models. Additionally, the ambient conditions cannot be controlled and are typically difficult to account for because of the difficulties in mounting equipment outside of the test wagon. For this reason, full-scale experiments typically foresee pressure taps as the only transducers installed on the tested wagons. It should be noted that full-scale methodologies to determine the direction and magnitude of wind speed have been proposed (26,75). ~~: see the works by Quazi et al. (26) or Bell et al. (75).~~

In Table 2 it is possible to see that full-scale experiments can also be used to measure the aerodynamic drag; this is done by interpolating and integrating the pressure coefficient of the front and base faces of the test wagon or by measuring the speed of the train as it coasting tests (48,49). The same procedure is not often employed for the estimation of side forces ~~(one example is the work by Bell et al. (75))~~. Measurements from these works are also often used to understand flow structures around the container (26,27). ~~(see Quazi et al. in (26) and (27)).~~

Full-scale tests are also often employed for the study of wind velocity in the slipstream and for the analysis of flow structures (this is done as a TSIs requirement for high-speed trains, but measurements on freight trains are also carried out during these campaigns, see Section 0). The data acquired with these methods can be harder to interpret because the measurement points are typically limited, and ambient wind conditions may influence the data. This limitation is less problematic to measuring slipstream flow velocity because the safety thresholds and measuring points to be used in this regard are dictated by the TSIs (11), although some works have raised doubts about their suitability concerning freight trains (70,76).~~, see Soper and Baker (76) and Gallagher et al. (70).~~ In

view of flow structures identification, full-scale tests are often supplemented by high-fidelity numerical methods like LES and its variants.

More frequently than full-scale experiments, wind-tunnel tests are conducted in a controlled environment on scaled, simplified models of the trains (the typical scaling factor ranging from 1:15 to 1:25). Wind-tunnel experiments allow control of the magnitude and yaw angle of the incident wind (represented as θ in Figure 3). This is the likely reason why they are the preferred method for investigating lateral forces on the test wagon in crosswinds (24,29–31,64) ~~(Alam and Watkins (30), Giappino et al. (24), Kocoń and Flaga (31), Giappino et al. (64) and Golovanevskiy et al. (29))~~ as well as the effect of crosswind on drag (29,38,64). ~~(Golovanevskiy et al. (29), Buhr et al. (38) and Giappino et al. (64)).~~

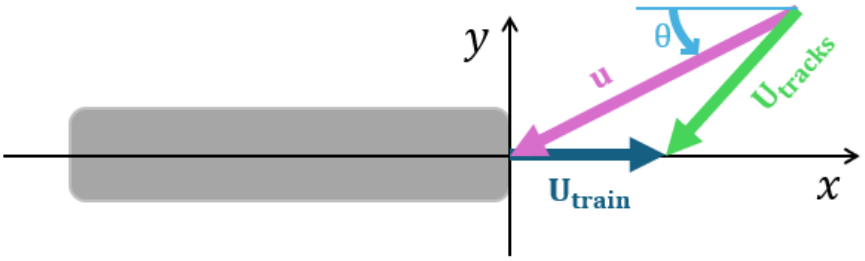

Figure 3, Representation of the yaw angle (θ) where u is the air velocity from the frame of reference of the train, U_{tracks} is the air velocity from the frame of reference of the tracks and U_{train} is the speed of the train.

Wind-tunnel experiments also find applications in the investigation of aerodynamic drag in no-crosswinds conditions, because they are cheaper than full-scale experiments while allowing better control of wind conditions, and do not require multiple runs of a moving-model rig. The main drawback of wind-tunnel tests is the non-similarity between the flow produced by the wind tunnel and the flow being investigated, since usually wind-tunnel tests are performed without the use of a

moving ground device. Nevertheless, this methods has been ~~Li et al. (3), Siegel et al. (25) and Buhr et al. (38) have~~ used ~~this method~~ to study the effect of gap size on the aerodynamic drag of intermodal container trains (3,25,38).

It should finally be noted in regard of wind-tunnel tests that previous research has shown that the use of a moving ground device does not significantly impact the force coefficients of model trains in crosswinds (65,72) ~~(see Bocciolone et al. (72) and Dorigatti et al. (65)),~~ although the flow is impacted over the entire height of the bogies, i.e., where the transversal speed is severely reduced by the stationary ground (67)~~., as shown by Premoli et al. (67).~~

Moving-model tests reproduce the relative movement between the model and the ground but, because of restrictions to the length of the rigs, they tend to have a very short time duration. Therefore, the tests need to be repeated multiple times and then an ensemble average is applied to the data from the runs, making sure that the measurements (taken originally over time) are aligned and scaled for differences in train speeds. The better similarity of moving-model tests compared to wind-tunnel tests performed on stationary models means that the former testing method is more suitable for studying slipstream velocity (39) ~~(Soper et al. (39))~~ and low-height flows, like the effect of embankment geometry (66). ~~(Noguchi et al. (66)).~~

Moving-model methods have been proposed that allow performing multiple measurements in a short time without neglecting the moving ground effects. ~~The~~ One such rotating rig ~~set up proposed by Gil et al.~~ (73) is composed of a model train running on a circular track. The set-up proposed by the authors has a diameter of 3.61 m and the train can run up to 118 rpm, corresponding to a speed of about 22 m/s. The advantage of a setup of this sort is that many measurements can be carried out in a short time while maintaining the moving ground conditions, but there are also disadvantages. The setup requires the use of models having a very small scale (e.g. 1:50 in ~~the work of Gil et al.~~ (73)) and this may affect the similarity of the flow but is necessary to avoid sharp discontinuities in the

orientation of each carriage. Additionally, the flow is obviously affected by the curvature of the path followed by the moving vehicles, especially with longer train models.

Both wind tunnels and moving models make use of train models scaled down with respect to the real train, resulting in smaller Reynolds numbers than in the real case. The flows, however, can be considered Reynolds-independent for values of the Reynolds number larger than approximately 250000 ~~0.25·10^6~~, as reported by a study on the dependence of the force coefficients on Reynolds number presented in ~~Alam and Watkins~~ (30).

A disadvantage of moving-model tests is the difficulty of studying the effect of crosswinds. The TRAIN rig in Birmingham makes use of fans to generate crosswinds in a section of the rail, so when the model reaches it, it will meet the incoming flow at a desired yaw angle. However, after disregarding the data collected in the first 1.27 m and in the last 0.64 m of the crosswinds section of the rig ~~(as suggested by Dorigatti~~ (63)~~)~~ only 4.44 m remain available for the analysis of measurements. ~~Soper et al.~~ ~~(39)~~ ~~studied~~ the effect of gap size on the overturning stability of an intermodal container train in crosswinds was studied using this rig (39). Another way to reproduce crosswinds effects in moving-model tests is to place the moving-model rigs in wind tunnels ~~(see Bocciolone et al.~~ (72)~~)~~. However, the same limitations are still present here as the size of the rig is confined by the dimensions of the wind tunnel.

It emerges from this section that the choice of the most suitable experimental method must be made with consideration to the specific topic of investigation and the objective of the study. Finally, it is crucial to remember that experimental data is also affected by error, due to the instrumentation but also the imperfect reproduction of the flow, as demonstrated by the fact that experimental methods often give different results.

3.2.2 Numerical methods

In this review, numerical methods are considered to be all those methods that evaluate the properties of the flow based on a physics-based mathematical/numerical model. This definition includes not only Computational Fluid Dynamics (CFD), but also the use of analytical formulas such as simplified drag formulas (see Section 0). These numerical methods are much less computationally demanding than CFD, and this has motivated their development for a variety of purposes and situations. Predictive formulae are available in the standards to calculate the overturning moment of a freight train in crosswind (EN 14067-6 (16)) and the pressure changes of the train-tunnel pressure signature, as well as the aerodynamic drag in tunnels (EN 14067-5 (15)). For more accurate predictions of the pressure waves in tunnels, 1D iterative methods have been devised (59–61), that can be run in seconds (while 3D CFD simulations would be likely to require at least days). Methods for an approximative simulation of the flow around bluff bodies suitable for the use on freight trains also exist. One of them is the 2D panel method, which has been adapted for viscous separated flows (71). ~~as was done in by Lai and Barkan (46) with the train energy model (TEM) subroutine proposed by the Association of American Railroads (AAR) in (52)~~. The numerical methods described above have the advantage of providing results quickly, at the expense of accuracy. Much more accurate (and expensive) numerical techniques are the 3D CFD methods. These ~~CFD~~ methods have some significant advantages over experimental ones; despite often being time-consuming due to the large computational effort required, they are easier to manage ~~and less time-consuming~~ as they do not require the physical production of scaled models and the use of a wind tunnel or setting up a line tests. ~~and,~~ Additionally, these methods allow the user to visualize the entirety of the flow in much greater detail (including post processing) compared to an experiment. It should be noted in this regard that techniques such as Particle Image Velocimetry (PIV) (25) or smoke streaks allow for the visualization some flow variables (e.g. instantaneous velocity) in experimental tests, but only in limited preselected locations.

Different CFD methods are available, each one having specific strengths and drawbacks. The most accurate method is Large Eddy simulation (LES) but it is also the most computationally expensive, this is why variants of this method have been proposed that use LES only in a portion of the domain and use the traditional Reynolds Averaged Navier-Stokes (RANS) methods elsewhere. The most popular variants of LES are Embedded LES (ELES), Detached Eddy Simulation (DES) ~~proposed by Strelets and Allmaras~~ (56) and further developed ~~by Spalart et al.~~ (57) and named Delayed DES (DDES). Methods have been proposed in literature to reduce the computational cost of simulating long trains with LES (and hybrids) methods, such as using periodic boundary conditions on inlet and outlet. This method allows to simulate the flow around a container far from the nose or tail of the train with similar accuracy than a simulation of the entire train (55).

With reference to Table 2, it can be observed that this family of methods finds large use in the study of the flow field around passenger and freight trains and has been shown ~~by Wang et al. (41) and Maleki et al. (20)~~ to be able to predict the flow topology accurately (20,41). In the same paper, it is concluded that traditional RANS and Unsteady ~~Unstationary~~ RANS (URANS) methods fail at this task (primarily by overpredicting the length of the recirculation regions). It should be noted that different formulations of the URANS method have been proposed to improve its accuracy for aerodynamic design applications, such as the method proposed in ~~by Xu~~ (54). This method increases the mesh resolution where coherent turbulent structures are detected and was proven ~~by Garcia et al.~~ (23) to significantly increase the accuracy of the URANS solver in terms of its aerodynamic forces and flow topology prediction.

The high accuracy of this family of methods in predicting both flow topology and aerodynamic forces allowed researchers to compare aerodynamic forces under different flow conditions, but also to identify the flow structures that explain these differences. This has been done to study the impact of gap size in intermodal container trains on drag, initially without considering the effect of

crosswinds (21,22) ~~(Maleki et al. (21) and Östh and Krajnović (22))~~ and more recently also in crosswinds condition (51) ~~(Maleki et al. (51))~~. The same methods have been applied to assess the lateral forces on stationary and moving vehicles (28,69) ~~(Hemida and Baker (28) and Liu et al. (69))~~. It is noted in Table 2 that the higher accuracy of the LES method in reproducing the characteristics of the flow makes it more suitable for studying the effect of the slipstream velocity on people stability (5,36) ~~(Flynn et al. in (5) and (36)). To the authors' knowledge, this topic has never been studied using methods like RANS or URANS~~.

~~Despite being generally incapable of predicting flow topology, RANS and URANS methods have been shown to be suitable for the calculation of aerodynamic forces, although with lower accuracy compared to LES.~~ Based on the aim of the analysis, different numerical techniques can be used, corresponding to different trade-offs between computational effort and accuracy. ~~The RANS method has been shown to be generally less accurate than LES and its variants, both in predicting the flow topology and the aerodynamic forces.~~ In particular, the use of ~~these~~ less computationally intensive approaches such as RANS is adequate for a comparative evaluation of the aerodynamic ~~performance~~ forces ~~of~~ for different geometries ~~(Maleki et al.~~ (20)~~),~~ whilst significant improvements in accuracy can be achieved using the URANS (20) technique. The best level of accuracy can be achieved using the LES method, but at the expense of considerable computational effort. Despite their limitations, ~~these~~ RANS and URANS methods remain widely used in the industry because of the very high computational costs of LES methods. ~~Iliadis et al. (33) used RANS~~ RANS has been used to study the drag of a freight train in a tunnel using the sliding mesh technique (33), and ~~while Zhang and Wang (85) used this method~~ to study the pressure waves generated at the intersection of two high-speed freight trains (85).

One final CFD method worth mentioning is Scale Adaptivece Simulation (SAS), this is another "hybrid" method that selectively and locally switches from URANS to LES. This method has

been shown to be more accurate than URANS, although less accurate than ELES, and has a computational cost of about 50% compared to ELES for both passenger trains and freight trains (20,41) ~~(Wang et al. (41) and Maleki et al. (20) respectively)~~. Although promising, this method at its present stage of development, struggles to switch from RANS to LES in the appropriate regions when the flow is not strongly globally unstable. This could be the reason why the method has found almost no use in literature.

Some remarks can be made about the use of CFD in literature. The most frequently used turbulence model for the URANS method is the k-ω SST (20,21,33,36,44,51,68), while for LES method (and its variants) the Smagorinsky model is also often used (22,28,36). It is common practice in CFD studies in literature to present mesh independence studies, however a rigorous method to assess the convergence is rarely used. Experts (90) and journals (91) recommend the use of the grid convergence index (GCI) for the assessment of numerical uncertainty.

4. Overview of past research results

~~Past research on freight train aerodynamics focused on some specific phenomena that mostly impact the energy-efficient and safe operation of freight trains. The main findings of past research are summarized in this section~~. ~~In this regard,~~ This section summarizes the main findings of research performed on freight train aerodynamics. It is worth ~~recalling~~ mentioning that past research ~~on freight train aerodynamics~~ was mostly concerned with intermodal container trains, therefore the results described below shall be considered, at least in strict terms, only applicable to this train type, whilst the investigation of aerodynamic effects for other freight wagon geometries remains to a large extent a subject open for future research. ~~Hereafter,~~ For intermodal container trains, the effect of inter-container gaps turns out to be of particular interest. Therefore, to support quantitative statements, below in the paper the size of the gaps is parametrized to the dimensions of the containers, labeled as

follows: *Lc* is the length of the container, *Wc* is the width of the container and *Hc* is the height of the container.

4.1 Aerodynamic forces on the vehicle

When a train is moving in the air, a resultant aerodynamic force will arise~~, all the components of this force are of interest in different respects~~. The drag force ~~points along~~ acts opposite of the direction of motion of the train and affects directly the mechanical power required to maintain the train in motion at a constant speed, and hence energy consumption involved with train motion. The side and lift forces, instead, impact the safe operation of the train because, if not managed properly, they may cause the derailment or overturning of the wagons. These aspects are discussed separately in the section below.

4.1.1 Drag

In intermodal container trains, the flow that takes place in the gap between containers directly affects the pressure on their surfaces. Consequently, the topology of the flow in the gap influences the (pressure) drag that the containers are subject to.

Increasing the gap size will always increase the drag coefficient on the two containers located upstream and downstream of the gap (i.e. the container facing the airflow first is upstream, and the one behind it, is downstream). However, the downstream container will be affected much more severely (3,21,22,24,25,38,46,53) ~~(Li et al. (3), Maleki et al. (21), Östh and Krajnović (22), Giappino et al. (24), Siegel et al. (25), Buhr et al. (38), Lai and Barkan (46)).~~ At gap sizes smaller than a critical length (between 0.5*Wc* and 1.0*Wc* approximately) two symmetrical vortices have a shielding effect on the gap, preventing the shear flow from impinging on the front face of the downstream container ~~(see section 4.2)~~ and resulting in the lowest drag coefficients. The critical gap size below which flow impingement is negligible is between 0.5*Wc* and ~~1.04*Wc*~~ 1.0*Wc* depending on the source (21,22,25) ~~(see Östh and Krajnović (22), Siegel et al. (25) and Maleki et al. (21))~~, but the scatter between the

results is more likely to be a consequence of the limited number of gap sizes tested in the different works rather than a substantial discrepancy between the flows investigated.

As the gap grows, the flow undergoes a regime change and impinges more and more in the gap, impacting the front face of the container downstream of the gap, increasing the drag dramatically. The steepest increase in the overall drag on the train is observed somewhere between ~~1.77*Wc*~~ 1.8*Wc* and 4.0*Wc* depending on the source (3,21,25,27,38) ~~(Siegel et al. (25), Buhr et al. (38), Li et al. (3), Maleki et al. (21), Quazi et al. (27)).~~ This means that the reduction of gap sizes in this range provides the largest advantage in terms of energy savings.

The drag continues to grow with the size of the gap and then plateaus to the maximum value of drag coefficient. This happens when the gap size reaches approximately 7*Wc* ~~(see Siegel et al. (25))~~ but the value of the drag coefficient never reaches the same value as that of a single container wagon in free flow.

Finally, it should be mentioned that the number of cars needed to measure force coefficients of a test wagon unaffected by the proximity of the nose and tail is not yet well understood. ~~Golovanevskiy et al. (29) suggested~~ It has been proposed in the literature (29) that 8 wagons (and a locomotive) are sufficient to allow the development of the boundary layer for the purposes of measuring the force coefficients of the middle cars (fourth and fifth). However, full-scale experiments ~~by Quazi et al.~~ (27) measured drag coefficients approximately 50% lower than previous LES (20) and wind-tunnel studies (3) ~~(respectively, Maleki et al. (20) and Li et al. (3))~~. The greater distance of the test wagon from the train nose was proposed as the main explanation for the discrepancy, suggesting that the stabilization of the boundary layer is not yet completely understood.

4.1.2 Drag in crosswinds

Crosswinds affect the topology of the flow; therefore, they obviously also affects the drag of wagons. ~~For small yaw angles (less than 5°) the drag coefficient is similar to the one in no-crosswind condition,~~

~~the minimum drag is still obtained with the smallest gaps on both sides, and the presence of an upstream wagon proves beneficial for the drag coefficient (this remains true up to yaw angles of 60-70°, as shown by Giappino et al. (24)).~~ At small yaw angles, the gap interval corresponding to the maximum rate of drag increase is the same as that described before, approximately between $1.8Wc$ ~~$1.77Wc$~~ and $3.2Wc$ ~~$3.23Wc$~~. However, for yaw angles exceeding 10 degrees, the interval of maximum drag gradient is approximately between $0.3Wc$ and ~~$1.77Wc$~~ $1.8Wc$ ~~(Maleki et al. (51))~~.

In the presence of crosswind gap size and yaw angle both influence the drag, as shown in Figure 4. Full-scale measurements showed that, for a given gap size combination, the drag coefficient increase with yaw angle follows a quadratic fit ~~(Quazi et al. (26))~~ and larger gaps cause a faster growth of the drag ~~(Quazi et al. (27))~~. Because no direct measurement of crosswinds was possible with the methodology of these works, the relationship obtained depends on the accuracy of the correlation between the yaw angle and flow asymmetry ~~as described by Quazi et al.~~ (26). These findings are consistent ~~with those of Buhr et al.~~ other findings in the literature (38). The specific quadratic relations are dependent on gap size~~, for an example of application of this technique the reader should consult Quazi et al.~~ (27).

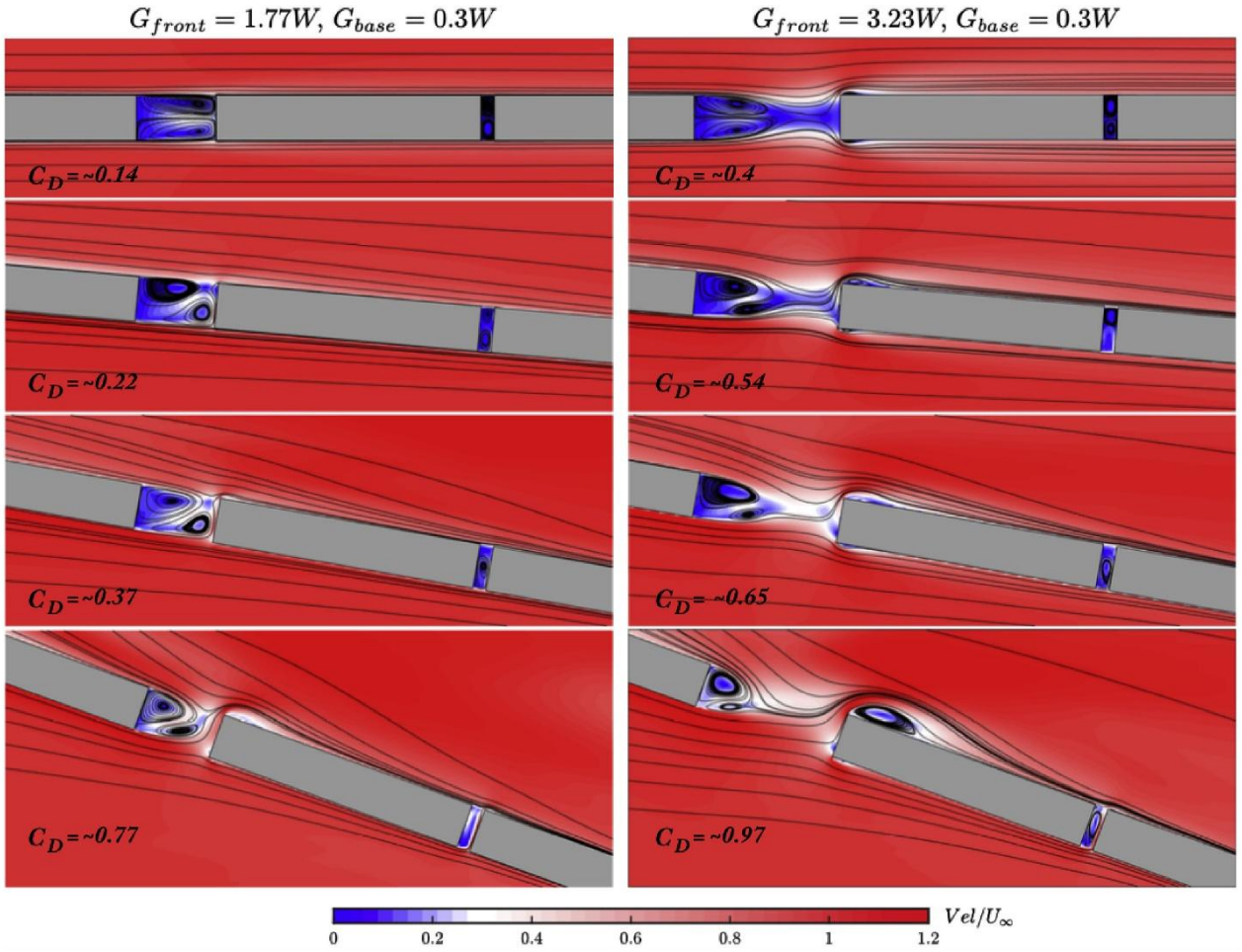

Figure 4, Effect of gap size and yaw angle on the impingement of the mean flow inside the gap between containers ~~(from Maleki et al.~~ (51)~~)~~.

For very large yaw angles (from 60° to 70° (24)) the upstream container no longer has a shielding effect on the flow inside the gap between containers. At these yaw angles, the presence of the upstream container does not reduce the value of the drag coefficient on the container downstream of the gap.

4.1.3 Recommendations for efficient operation of freight trains

Gaps are the main source of drag for intermodal container trains, therefore large gaps like those occurring when a wagon is left empty must be avoided whenever possible (3,25) ~~(see for example Siegel et al.~~ (25)~~ and Li et al.~~ (3)~~). Large gaps~~ Empty wagons (or gaps as large as the length of the container) are so detrimental to the drag that ~~the addition of an empty container in place of an~~ loading

an empty container on the ~~empty~~ wagon is justified in terms of energy consumption, because the increase in the overall train resistance due to the addition of the container's weight is offset by the reduction of the aerodynamic drag (46,47) ~~(Lai and Barkan (46) and Beagles and Fletcher (47))~~.

A similar advantage can be found in double stacked intermodal container trains when an empty wagon stands between two fully loaded ones. In this case, moving one of the containers from the adjacent double-stacked wagons to the empty one results in a drag reduction of as much as 35% ~~(Maleki et al. (21))~~

Finally, the gaps between containers should be as small as possible, especially if their size falls in the 1.8-4.0Wc range where the steepest drag gradient occurs. As discussed in the previous sections, in no-crosswind conditions the highest drag gradient occurs for gaps between 1.8Wc and 4.0Wc approximately~~, however, this is not the most realistic case~~. If the air is not stationary, the most likely scenario is to travel with at least a small yaw angle, especially at the modest speed of freight trains. Therefore, it is advisable to maintain the size of the gap under ~~1.77Wc~~ 1.8Wc, to avoid the gap interval of steepest gradient of drag for weak crosswind conditions (38,51)~~(see the results of Maleki et al. (51) and Buhr et al. (38)).~~

4.1.4 Quantifying the drag coefficients

Given the importance of aerodynamic drag for the energy-efficient operation of freight trains, researchers have made attempts to predict the drag coefficient by means of simple formulas. All of these formulas make use to some extent of experimental data, which is to be expected given the complexity of the phenomena involved.

Predicting the aerodynamic drag is important because it contributes to the overall running resistance of the train. This is usually defined as having a constant component (attributed to rolling resistance and slope), a component linear with train speed (attributed to mass-related speed-dependent

mechanical friction) and a component quadratic with speed caused by aerodynamic drag (49). These three components are summarized in Davis equation (19), see Eq. (2),

$$F_D = A + BU_{train} + CU_{train}^2 \quad (2)$$

Where F_D is the overall running resistance force, U_{train} is the speed of the train, and A, B and C are the coefficients of the polynomial expression. Methods on how to estimate the coefficients (A, B and C in Eq.5) are available in the literature (40,48,49). ~~of the overall resistance to motion the reader may consult Lukaszewicz (40), Rochard and Schmid (48) and Somaschini et al. (49).~~

Despite the importance of understanding the behavior of the drag resistance for increasing distance of the wagon (45,50) ~~(see Engdahl et al. (50) or Lai et al. (45))~~ from the nose, the complexity of the problem makes it very challenging to find a formula that would be general to all freight trains; therefore, some researchers aim instead at predicting the drag on the entire train under some simplifying assumptions. One such formula is a best fit of experimental data to calculate the drag coefficient of an intermodal container train in an open straight track with different gap sizes and yaw angles ~~An example of a law that attempts to account for both gap size and yaw angle~~ (valid for yaw angles below 60°, and provided that all gaps are of equal size), is the one ~~proposed by Beagles and Fletcher (47),~~ presented in Eq. (3) (47). The reference area is taken to be 10 m^2.

$$C_{D,train} = \frac{1 + 2\left(1 - e^{-6\theta}\right)}{3} C_{long} + \frac{1}{2}\mu C_{lat} \quad (3)$$

Where C_{long} and C_{lat} are defined in Eq. (4) and Eq. (5) respectively and μ is the coefficient of friction between the rail and the wheel.

$$C_{long} = (0.56 - 0.16\cos 6\theta)\left(1 - e^{(0.919\cos\theta - 1)G}\right) - 0.003L \quad (4)$$

$$C_{lat} = 0.46L\theta^2 \quad (5)$$

Where G is the size of the gaps and L is the length of the wagons and θ is the yaw angle. Eq. 2 is one of the few proposed laws that consider the friction between rails and wheels caused by the side force, see the second term.

Other works investigated the relation between drag coefficients on containers and the gap size between containers. Studies that investigate the change in drag coefficient on a test container mounted on a simplified, model-scaled intermodal container train in 0° and 5° yaw angle (38). The results of these measurements with different container gaps upstream and downstream of the test container are summarized in Figure 5, it should be noted that the upstream gaps have been varied while keeping the downstream gap at $0.3Wc$ and the downstream gaps have been varied while keeping the upstream gap at $0.3Wc$.

~~Other works that present the relation between drag coefficients of wagons and the gap size between containers are Buhr et al. (38) (see Figure 5) and Li et al. (3) (see Figure 6). The varying gap sizes considered by Buhr et al. (38) vary only one at a time (meaning that the upstream gap size varies at a constant downstream gap size of 0.3Wc and the downstream gap size varies at a constant upstream size of 0.3Wc).~~

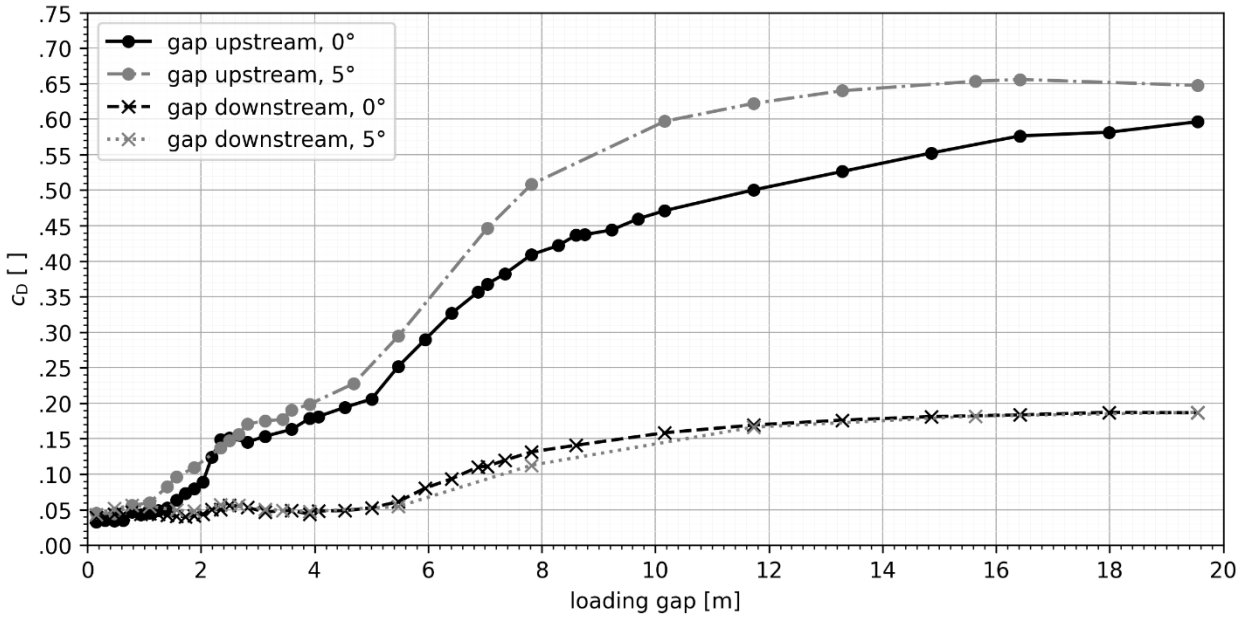

Figure 5, Change in container drag coefficient with varying upstream (downstream) gap while downstream (upstream) gap remains constant at 0° and 5° yaw angles ~~Aerodynamic drag coefficient of test container for gap upstream and gap downstream at 0° and 5° crosswind condition (Buhr et al.~~ (38)~~)~~.

In reference (3), wind-tunnel experiments are used to measure drag resistance on a test container while varying the upstream and downstream gaps. The results are show in in Figure 6 in terms of drag coefficient vs. gap size, for downstream and upstream gaps having the same size.

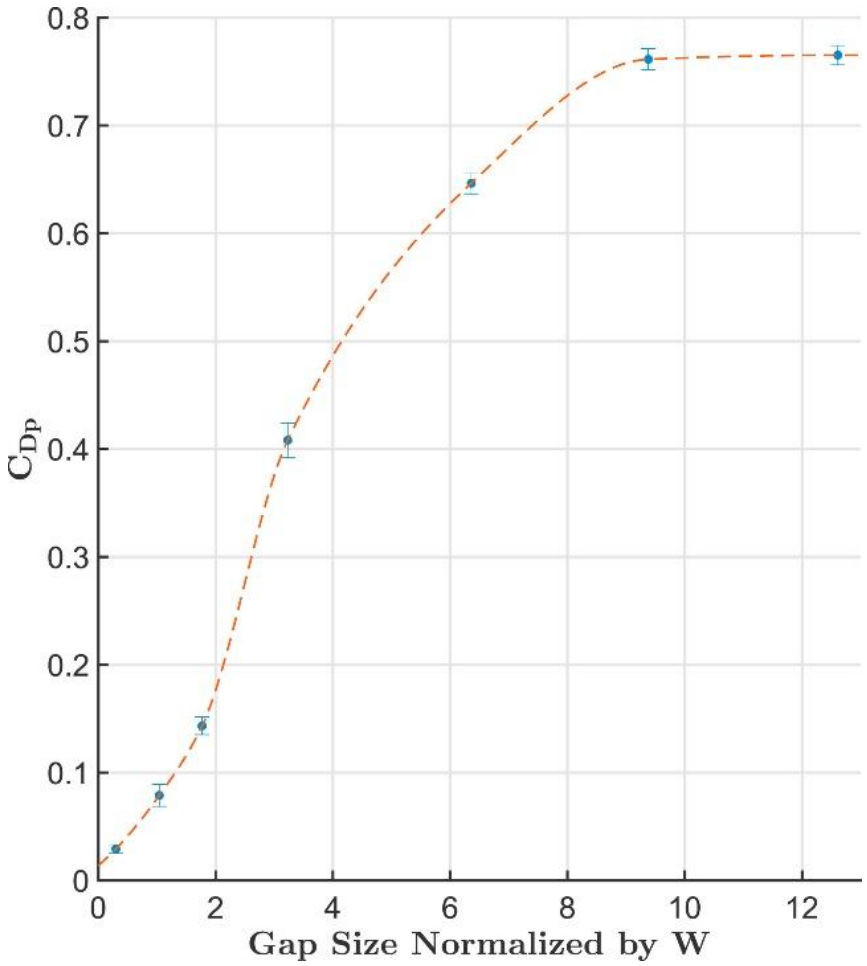

Figure 6, Change in pressure drag coefficient of a container in an intermodal container train with varying upstream and downstream inter-container gaps of equal length in no-crosswinds conditions (3). ~~Pressure drag coefficient with upstream and downstream gap size are the same, no-crosswind (see Li et al. (3)).~~

~~As a final remark, it is important to recall that aerodynamic drag is only important insofar as it contributes to the overall vehicle resistance, so relations to quantify this latter force are also useful. For methods of estimating the parameters of Davis equation (see Eq. (5)) for the overall resistance to motion the reader may consult Lukaszewicz (40), Rochard and Schmid (48), Somaschini et al. (49).~~

$$F_D = A + BU_{train} + CU_{train}^2 \quad (5)$$

Where F_D is the overall resistance to motion of the train, U_{train} is the speed of the train, and A, B and C are the coefficients of the polynomial expression.

4.1.5 Effects of crosswinds on aerodynamic forces

Although the largest component of the aerodynamic force experienced by a vehicle is drag, the other components are also of interest to designers and operators both for matters of safety and efficiency. The side and lift forces are a subject of study in train aerodynamics because they contribute to the moment about the contact point between the wheels on the leeward side of a train and the rails (overturning moment), see Figure 7. This is not a problem for heavy locomotives, but is of particular importance for freight wagons, because trains for which the weight of the empty wagon is very low compared to laden wagons and to passenger vehicles (92). Very important tools to assess the overturning risk for rail vehicles due to aerodynamic forces are CWCs (see definition in Section 0) even if they have not been widely used, given the low speed of freight trains. The overturning risk is mainly related to strong winds at high angle of attack, rather than for the relative speed and small angle of attack like for high-speed trains (93). The risk of crosswinds is also made more severe when the vehicle is subjected to a sudden gust of wind. The effect of the build-up time of the gusts on overturning risk has been studied and it was found that the unloading of the leeward wheels is most critical for gusts of a build-up time smaller than 1s (92).

In addition to the overturning moment, the side force is worth some consideration on its own, since an alternative way in which a train may incur an accident is derailment, which occurs when one or more wheels climb over the rail and fall out of the track to the field side.

While both yaw angle and gap size contribute to increase the side force and the overturning moment, the yaw angle has been found to be the dominant effect (Maleki et al.(51)). The roll moment experienced by a container is generally greater when the loading efficiency (the ratio between the

occupied container spots and the total container spots) is low, but not all containers are equally affected. The risk of overturning related to the loading conditions of the wagons and to the presence of empty wagons and container wagons has been investigated and it was found that containers on trains of equal loading efficiency experience greater coefficients of lift and roll moment when they are preceded by an empty wagon than when they are followed by one ~~(Soper et al. (32)), therefore wagons downstream of large gaps should be considered critical also in regard of their stability~~. This finding suggests that wagons downstream of large gaps should be considered at most severe risk with regard to their stability (93).

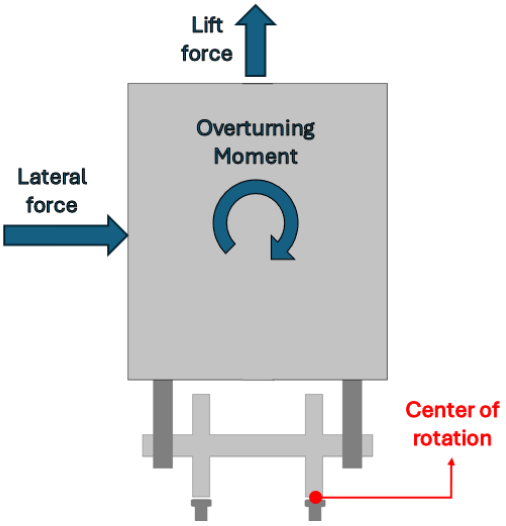

Figure 7, Contribution of lift and lateral force to overturning moment.

The situation in which a container is subject to the lowest overturning moment is the one in which it is preceded by a loaded wagon but followed by an empty one ~~(Giappino et al. (24))~~. This condition of course cannot be realized for all containers, so the overall best condition for the whole train in terms of overturning moments caused by aerodynamic forces remains the one with greater loading efficiency.

Finally, it should be noted that crosswinds are not the sole cause of overturning accidents. More frequently, other factors such as centrifugal acceleration, uneven tracks and the dynamic behavior of suspensions can lead (together with crosswinds) to overturning (37,62,92).

4.2 Slipstream Characteristics

Freight train slipstreams can be dangerous for bystanders (passengers on platforms or railway workers). Additionally, a strong slipstream is connected to higher drag because, for the air to be set in motion, momentum needs to be transferred from the vehicle to the surrounding air at a higher rate.

To quantitatively compare the slipstreams caused by freight trains, with their diverse and complex geometries, two parameters are reported in the TSIs (11) and European standards (EN 14067-4 (14)). One is the upper limit of the 95% confidence interval for the velocity horizontal magnitude during the entire passing of the train or in its wake, denoted as $u_{95\%}$, and the other is the upper limit of the 95% confidence interval for the peak-to-peak pressure changes during the entire passing of the train or in its wake, denoted as $\Delta p_{95\%}$. The slipstream velocity $u_{95\%}$ and the slipstream peak-to-peak pressure change $\Delta p_{95\%}$ are calculated according to Eq. 6 and Eq. 7 respectively, from EN 14067-4 (14).

$$u_{95\%} = \bar{u}_{max} + 2\sigma_u \tag{6}$$

$$\Delta p_{95\%} = \overline{\Delta p}_{max} + 2\sigma_p \tag{7}$$

In Eq. 6 $\bar{u}_{max}$ and σ_u are respectively the mean value and standard deviation of all maximum values reached in the individual runs by the horizontal air speed component subjected to 1 s moving average. Similarly, in Eq. 7 $\overline{\Delta p}_{max}$ and σ_p are respectively the mean and the standard deviation of the maximum peak-to-peak pressure changes. The TSIs requires that measurements for slipstream velocity are made at a distance of 3.00 m from the center of the track (COT) at the heights of 0.20 m and 1.40 m from the top of the rail (TOR), while the pressure change measurements should be made a distance of 2.50

m from COT between 1.50 m and 3.00 m from TOR in increments of 0.30 m. All measurements need to be made with a maximum crosswinds speed of 2 m/s (TSIs (11)).

4.2.1 Slipstream characteristics under weak crosswinds

Various measurements have been made to characterize the slipstream around freight trains and a significant agreement was reached on the point that a subdivision of the slipstream in four regions should be considered as previously proposed in literature ~~Baker et al.~~ (80): the nose region, the boundary layer region, the near wake region and the far wake region. Consistently with common nomenclature in literature, the pressure coefficient is here denoted as *Cp*, the longitudinal component of the velocity normalized by the speed of the train is denoted as *U*, and the transversal and vertical components are denoted as *V* and *W* respectively.

The nose region (or upstream region) is a region where a sharp peak in velocity and pressure in the slipstream can be identified with high repeatability, to the point that the flow can be considered inviscid in this region. In a wind-tunnel test with a class 66 locomotive ~~Soper et al.~~ (39) it was found that this region extended up to 18.75 m from the nose of the train (full-scale dimensions), while a DDES analysis ~~performed by Flynn et al.~~ (36) identified the inviscid region to be from 2 m upstream of the train nose to 10 m downstream of it. In this region, there is a positive peak in the pressure coefficient, followed by a negative one of greater magnitude ~~(Soper et al. (39))~~. A positive peak is also observed in the magnitude of the velocity corresponding to the passage of the train nose. At the sides of the train, this peak in magnitude can be mainly attributed to an increase in *U* and *V*, while on top of the train it is mainly attributed to *U* and *W*, consistently with regions of flow separation at the corners of the front face of the locomotive (36,79) ~~(Bell et al. (79), Flynn et al. (36)).~~

After the nose region, the boundary layer region begins. Here the pressure coefficient undergoes a series of positive and then negative peaks similar to the one corresponding to the passage of the nose of the train, but smaller in magnitude. These smaller peaks are due to the gaps between

wagons and, therefore, are larger when the gaps between containers are larger (39,79) ~~(Soper et al. (39), Bell et al. (79))~~. In freight trains, the velocity magnitude in the boundary layer builds up gradually across the length of the train, hindering the identification of the nose peak. In contrast, for passenger trains a peak of the velocity magnitude is clearly visible and the magnitude of the velocity reaches a stable value almost immediately after the nose ~~(Sterling et al. (6))~~.

One way to quantify the development of the boundary layer is the displacement thickness (δ^*). This quantity is defined in Eq. 8 and it represents the distance from the surface that would enclose a flow of an inviscid fluid at uniform freestream velocity with the same flow rate than the real flow. It depends mainly on the distance from the train nose.

$$\delta^* = \int_0^\infty \left(1 - \frac{U}{U_{train}}\right) dy \tag{8}$$

Where y is the distance from the surface.

A consensus about the length after which the displacement thickness (and thus the development of the boundary layer) stabilizes has not been reached in literature. Wind-tunnel experiments ~~by Soper~~ (37) show a boundary layer growth up to 100 m from the nose, with δ^* ranging between 0.6 and 1.4 m, while full-scale measurements ~~by Bell et al.~~ (35) suggested that the displacement thickness stabilizes at a value of about 1 m at about 200 m from the nose of the train. This question is also made more difficult by the variability in freight train geometry: full-scale slipstream measurements (81,82) indicate that the boundary layer may be considered stable within four wagon lengths for loading efficiencies above 50% but only after the fifth wagon length when loading efficiency is lower than 50%. The repercussions of the development of the boundary layer on the drag have been described in Section 0. The boundary layer thickness is not noticeably affected by the presence of single large gaps (i.e., the situation typical of a single missing container), but the presence of multiple, smaller gaps (each with 2 m size at least) can reduce the size of the boundary layer.-

After the boundary layer region, near the end of the train, the near wake region begins. Several studies have identified the presence of two counter-rotating longitudinal vortices forming in the wake of smooth passenger trains, these often lead the peak velocity to be recorded in the near wake region (6,74,78) ~~(Soper et al. (78), Sterling et al. (6), Bell et al. (74))~~. This is different from the flow in the near wake of a freight train, in which the velocity decays into the far wake (which is found to begin approximately 100 m after the end of the train), and no peaks can be observed (6,39) ~~(Sterling et al. (6), Soper et al. (39))~~. The fall of slipstream velocity can be modeled with power-law type equations with the exponent set to -0.85 for freight trains ~~(Soper et al. (39))~~ and -0.5 for passenger trains ~~(Baker et al. (80))~~.

4.2.2 Slipstream characteristics under crosswinds

The increase in the slipstream velocity that can be attributed to crosswind is known as slipstream amplification. Full-scale measurements ~~by Bell et al.~~ (35) showed that even very modest crosswinds give rise to asymmetries in the slipstream. In this study, the authors observed that for yaw angles as low as 2° the flow around the trains were asymmetrical despite the symmetrical loading configuration.

Strong crosswinds affect the flow even more severely, pushing the slipstream on the windward side (the side facing towards the wind) against the train. ~~On the leeward side, the effect is the opposite, and the boundary layer thickness becomes enlarged by the effect of crosswinds. Bell et al. (35) reports values of displacement thickness ranging from 2 to 4 m in crosswind conditions, compared to 1-2.5 m in weak crosswind.~~ On the leeward side (the side facing away from the wind), the effect is the opposite, and the boundary layer thickness becomes enlarged by the effect of crosswinds. Displacement thickness ranges from 2 to 4 m in crosswinds conditions, compared to 1-2.5 m in weak crosswinds (35).

At heights below the flow on the roof (meaning below 4 m ~~from top of rail (~~TOR~~) in Flynn et al.~~ (30)), slipstream amplification only occurs on the leeward side, while no significant amplification

is observed on the windward side. In particular, the DDES analysis ~~by Flynn et al.~~ (5) showed that a severe slipstream amplification can occur on the leeward side of the nose region, making it a critical region of the slipstream regarding the safety of bystanders.

4.2.3 Stability of bystanders in slipstream

Strong slipstream velocities pose a challenge to the safety of passengers on platforms and railway workers because they risk losing balance because of the air flow. The slipstream velocity (see Eq. 6 ~~equation (6)~~) is one of the most important and most often used parameters to quantify this risk for passenger trains, but for freight trains the current TSIs do not prescribe any standardized threshold for this value. Freight trains can generate values of $\Delta p_{95\%}$ exceeding the threshold prescribed for passenger trains travelling at speeds up to 249 km/h, even when they travel at much lower speeds such as 85 km/h~~, see Flynn et al.~~ (36). In this same reference, values of $u_{95\%}$ close to the TSIs threshold are reached by freight trains.

The most critical region is again the nose-peak region, where the velocity magnitude of the flow reaches up to 120% of train speed. Scaling this result for the speed of 120 km/h (which is currently the maximum service speed for freight trains in the UK), these gusts would have sufficient intensity to cause people to lose balance ~~(Soper et al.~~ (39)~~)~~.

The slipstream caused by a freight train is typically more turbulent than the one generated by a passenger train. Correspondingly, the velocity values of 1 s gusts in the slipstream are considerably higher for freight trains compared to passenger trains, although still under the TSIs thresholds in the current range of service speeds ~~(Soper and Baker~~ (76)~~)~~.

4.3 Ballast flight

Ballast flight is the phenomenon in which ballast stones are projected by air flow from the ballast bed and hit the underbody of the train or the rail. This occurrence is understood to be the consequence of two consecutive events (9). ~~First~~ At first, the vibrations induced by the train cause the particle to be

set loose from contact with the other particles~~,. Then,~~ then the displaced particle encounters a wind flow ~~having~~ with enough momentum to carry it ~~(Jing et al.~~ (9)~~)~~. It should be noted that the mechanical and aerodynamic contributions are difficult to quantify, and several factors are at stake, including weather conditions and geometry of the particles. In this regard, a full-scale study ~~by Soper et al.~~ (86) concluded that in well-maintained tracks the mechanical and aerodynamic forces are of the same order of magnitude.~~, while~~ The same study showed that in poorly maintained tracks the mechanical contribution to vertical forces acting on particles is prevailing, leading to a substantial increase in the risk of initiating ballast flight.

Freight trains typically have rougher geometries in the underbody (especially compared with high-speed passenger trains), producing a highly turbulent flow between the track and the train. However, the velocity of freight trains is well below those typical for ballast flight (300 km/h or higher) so it remains unclear whether ballast flight will become a problem at the relatively modest speed of 160 km/h.

The investigation of this problem is particularly complicated: full-scale measurements of the underbody flow are expensive and difficult to perform, so scaled models and CFD methods are more often used instead (87). However, the particularly irregular geometries involved in these flows pose challenges for these methods too. ~~Soper et al.~~ ~~(87) compared.~~ Comparing the results of a moving-model train and CFD with full-scale experimental data (87) ~~and~~ it was found that a moving model can be used to replicate the flow velocity and pressure field between the train and the rail (although a particular upside-down rig had to be used). The CFD results instead were able to replicate the flow, but consistently overpredicted the pressure field: this finding has been explained by the fact that the surface of the ballast bed had been modelled as a flat plane, and thus ballast roughness considered in the simulation was lower compared to the real case, allowing the flow to conserve its total pressure ~~(Soper at al.~~ (87)~~)~~. Attempts have been made to formulate methodologies to address this issue. One

of these methods uses CFD with a sliding mesh to simulate the flows under the train while including the sleepers in the geometry of the tracks, instead of using a flat moving ground. The results show that the combined effect of strong vertical fluctuations at the height of the ballast bed and the lift induced by the pressure field could lift particles having a diameter up to 10 mm larger than previously thought ~~(Paz et al. (88))~~. LES simulations have also been used to address this same issue, attempting to simulate the underbody flow of a train using the scanned 3D surface of an actual ballast bed instead of a flat surface. As expected, a more chaotic and turbulent flow was found close to the ballast bed without major changes to the flow close to the train surface ~~(Paz et al. (83))~~.

4.4 Freight trains in tunnels

Another example of confined flow is the flow around trains in tunnels. In this situation, the train acts as a piston pushing the air out of the tunnel and creating a compression wave that travels to the opposite end of the tunnel. Depending on the length, the blockage ratio and the roughness of the train, a portion of the air may flow back in the opposite direction of the train because of the pressure gradient created by the piston effect, thus relieving some of the pressure built up at the nose. Freight trains ~~tend to have higher blockage ratios and~~ have rougher shapes than passenger trains, giving rise to a more severe piston effect ~~(Negri et al. (77))~~ and their sharp corners cause separation bubbles that effectively increase their blockage ratio (58). The gaps between containers play a role in the piston effect too, increasing the roughness of the train and favoring the pressure build-up in front of the train ~~(see Bell et al. (7))~~. Numerical 1D methods have been proposed and used in literature to carry out simulation of the propagations of the pressure waves within tunnels (59,60). The application of these methods to freight trains is sometimes problematic because of the bluff shape of the wagons and of the discontinuous blockage ratio. However, novel 1D methods have been proposed addressing these difficulties with improved accuracy (61).

The increase in pressure caused in front of the train because of the piston effect of trains passing through tunnels has the effect of increasing the drag of freight trains in tunnels. ~~Cross et al. (58) found that~~ Drag in tunnels is predominantly pressure drag, and the blockage ratio is a major factor in determining it (58). For a blockage ratio of 0.85 the drag was found to be 50% greater than for a train in open air when running at constant speed and the increase in drag was even more significant during train acceleration.

Slipstream effects raise safety concerns in tunnels too: in this regard, the magnitude of flow velocity that freight trains produce in the slipstream is different compared to conventional and high-speed passenger trains because the inhomogeneous shape causes discontinuous growth of the slipstream. As a result, the peak velocity for freight trains typically occurs near the nose, while it is in the near wake for passenger trains ~~(Negri et al. (77))~~.

Finally, the pressure field in the tunnel as the train passes by is also affected by the propagation of pressure waves and their reflections. A compression wave is created as the nose enters the tunnel and an expansion wave when the tail enters the tunnel. These waves propagate in the tunnels reflecting (with phase inversion) at each end until the energy is dissipated due to air viscosity. For freight trains, the maximum amplitude of the pressure wave is typically reached in correspondence to the initial compression wave, but if the loading efficiency is low (33%) ~~in the simulation by Iliadis et al. (34))~~ then other peaks are present, suggesting that one-dimensional models may be unsuitable for this analysis (34).

5. Open points and further research

As outlined in previous sections, the rough shapes of freight wagons and locomotives have important repercussions on many aerodynamic aspects that cannot be ignored if freight trains must be operated at high speed. The strongly turbulent and transient nature of the flow makes the use of both numerical

and experimental methods particularly challenging. Consequently, some questions concerning freight-train aerodynamics remain open at present and are outlined in this section.

It is evident from the analysis of the scientific literature that research on freight-train aerodynamics has so far mostly addressed intermodal container trains (with few exceptions (42,43,68,81,82,84,89)) ~~(among the few exceptions, Nayeri et al. (42) and Watkins et al. (43))~~. One reason for this is that intermodal freight transportation takes the largest share of rail freight transport. However, this fact alone does not justify scarce interest in the aerodynamics of other freight train types, given that the intermodal share of rail freight transport ranges from 10% to 45% in European countries, which means that in all likelihood the study of aerodynamic effects remains presently unaddressed for the majority of the transported freight (in terms of tonnage times mileage) (18). To understand the global impact of an increase in the speed of freight trains, a more comprehensive approach is needed, encompassing other freight train types.

Data on the prevalence of wagon types needs to be considered when selecting the train geometries for future studies, especially for goods that would benefit from high-speed rail transport, such as low-density high-value goods (4) ~~[3]~~. Additionally, trains are not always composed of only one wagon type, therefore models with realistic mixed compositions ~~(such as those in the geometry database proposed by Corniani et al. (89))~~ should be studied to understand the impact of diverse wagon geometries on the flow while still focusing on cases of practical interest for operators.

It is standard practice in both numerical and scaled experimental investigations to simplify the geometry of the model, and one hypothesis that is ubiquitous in these works is that container corrugation does not affect the overall flow, so cuboids with flat surfaces are used to replace the actual geometry of the containers. To the knowledge of the authors, no works exist in the literature that investigate the impact of the container corrugations on the flow, despite the contribution that the increased roughness of the surface could have on the flow in the slipstream. Regarding this point, as

discussed in section 0, ~~a recent work by Quazi et al. (27) provided a practical case in which~~ CFD simulations and wind-tunnel tests can largely overpredicted the drag coefficient of a full-scale test wagon (27).

Finally, further research is needed to understand the stabilization of the boundary layer and of the drag coefficient, specifically at what distance from the nose of the train they can be considered stabilized. In section 0, different indications are provided for the length at which the boundary layer stabilizes and their impact on drag is discussed.

5. Conclusions

This review provides a summary of the State-of-the-art on the aerodynamics of freight trains. It can be stated that research in this field has been so far mostly focused on intermodal container trains, so the applicability of the results presented here to other types of freight trains is questionable.

Significant efforts have been made to study the aerodynamic forces on freight trains, some robust findings emerge from the literature, but other points remain open. The most important point of consensus is the general desirability of keeping small gaps between containers, to reduce drag resistance and mitigate overturning and derailment risk (as reflected in the recommendations listed in section 0). More research is needed, instead, to understand the relation between slipstream and drag, and particularly at what distance from the nose of the train can the slipstream and the drag be considered stable. Flexible and fast tools for the estimation of the drag in realistic conditions (different geometries, varying gap sizes, yaw angle, etc.) would be highly desirable, and some attempts were made to define simple analytical formulas fitting the results of experimental and numerical analyses. However, the complexity of this task is such that none of the proposed laws has found wide application so far.

Safe operation of freight trains requires not only the mitigation of the aerodynamic forces acting on the train, but also of the slipstream and pressure build-up in tunnels. The bluff shapes of freight

trains cause greater slipstream velocities, leading to greater risk for people standing near the railway line. Given that the service speed of freight trains has always been relatively low, the TSIs do not prescribe any regulation concerning the slipstream of freight trains. However, results from section 0 suggest that if the speed of freight trains is increased to the target value of 160 km/h, slipstream effects would represent a substantial risk to bystanders. It is then expected that the elaboration of regulations concerning the slipstream effects for freight trains will be needed in the near future.

Acknowledgments

The research reported in this paper has received funding from the European Union's Horizon Europe research and innovation program under grant agreement: HORIZON-ER-JU-2022-ExplR-04. Views and opinions expressed are however those of the authors only and do not necessarily reflect those of the European Union or Europe's Rail Joint Undertaking. Neither the European Union nor the granting authority can be held responsible for them.

Funding statement

The research reported in this paper has received funding from the European Union's Horizon Europe research and innovation program under grant agreement: HORIZON-ER-JU-2022-ExplR-04

References

1. White paper on transport – Roadmap to a single European transport area – Towards a competitive and resource efficient transport system [Internet]. 2011. Available from: http://europa.eu
2. Deutsche Bahn 2022 Integrated Report. 2022.
3. Li C, Burton D, Kost M, Sheridan J, Thompson MC. Flow topology of a container train wagon subjected to varying local loading configurations. Journal of Wind Engineering and Industrial Aerodynamics. 2017 Oct 1;169:12–29.

4. Boehm M, Arnz M, Winter J. The potential of high-speed rail freight in Europe: how is a modal shift from road to rail possible for low-density high value cargo? European Transport Research Review. 2021 Dec 1;13(1).

5. Flynn D, Hemida H, Baker C. On the effect of crosswinds on the slipstream of a freight train and associated effects. Journal of Wind Engineering and Industrial Aerodynamics. 2016 Sep 1;156:14–28.

6. Sterling M, Baker CJ, Jordan SC, Johnson T. A study of the slipstreams of high-speed passenger trains and freight trains. Proc Inst Mech Eng F J Rail Rapid Transit. 2008;222(2):177–93.

7. Bell J, Henning A, Volkert R, Michael O, Renschler C, Siegel L, et al. The Influence of Gaps Between Containers on Pressure Increase Along Freight Trains in Tunnels. In: Proceedings of the Sixth International Conference on Railway Technology: Research, Development and Maintenance. Civil-Comp Press; 2024. p. 1–13.

8. DB Freight Wagons catalog v2011 [Internet]. Deutsche Bahn (DB). 2011 [cited 2025 Jul 8]. Available from: https://nl.dbcargo.com/resource/blob/1430008/9767e97bb070ccbbf77efd84e7d64948/freight_wagon_catalog_v2011-data.pdf

9. Jing G, Ding D, Liu X. High-speed railway ballast flight mechanism analysis and risk management – A literature review. Vol. 223, Construction and Building Materials. Elsevier Ltd; 2019. p. 629–42.

10. Hemida H. Contribution of computational wind engineering in train aerodynamics—past and future. Journal of Wind Engineering and Industrial Aerodynamics. 2023 Mar 1;234.

11. Commission Regulation (EU) No 1302/2014 concerning a technical specification for interoperability relating to the 'rolling stock — locomotives and passenger rolling stock' subsystem of the rail system in the European Union [Internet]. Nov 18, 2014. Available from: https://eur-lex.europa.eu/eli/reg/2014/1302/oj/eng

12. EN 14067-1 Railway applications - Aerodynamics - Part 1: Symbols and units. CEN; Apr, 2003.
13. EN 14067-3 Railway applications - Aerodynamics - Part 3: Aerodynamics in tunnels. CEN; Apr, 2003.
14. EN 14067-4 Railway applications - Aerodynamics - Part 4: Requirements and test procedures for aerodynamics on open track. CEN; Dec, 2018.
15. EN 14067-5 Railway applications - Aerodynamics - Part 5 Requirements and assessment procedures for aerodynamics in tunnels. CEN; Dec, 2021 p. 98.
16. EN 14067-6 Railway applications - Aerodynamics - part 6: Requirements and test procedures for cross wind assessment. CEN; Jul, 2018.
17. BSL Transportation Consultants. Combined Transport in Europe. Paris; 2019.
18. International Union of Railways. 2020 Report on Combined Transport in Europe. 2021.
19. Davis WJ. The tractive resistance of electric locomotives and cars. General Electric; 1926.
20. Maleki S, Burton D, Thompson MC. Assessment of various turbulence models (ELES, SAS, URANS and RANS) for predicting the aerodynamics of freight train container wagons. Journal of Wind Engineering and Industrial Aerodynamics. 2017 Nov 1;170:68–80.
21. Maleki S, Burton D, Thompson MC. Flow structure between freight train containers with implications for aerodynamic drag. Journal of Wind Engineering and Industrial Aerodynamics. 2019 May 1;188:194–206.
22. Östh J, Krajnović S. A study of the aerodynamics of a generic container freight wagon using Large-Eddy Simulation. J Fluids Struct. 2014 Jan;44:31–51.
23. García J, Muñoz-Paniagua J, Xu L, Baglietto E. A second-generation URANS model (STRUCT-ε) applied to simplified freight trains. Journal of Wind Engineering and Industrial Aerodynamics. 2020 Oct 1;205.

24. Giappino S, Melzi S, Tomasini G. High-speed freight trains for intermodal transportation: Wind tunnel study on the aerodynamic coefficients of container wagons. Journal of Wind Engineering and Industrial Aerodynamics. 2018 Apr 1;175:111–9.

25. Siegel L, Buhr A, Bell J, Henning A. Analysis of Flow Structures in Different Loading Gaps of Freight Trains. In: Pombo J, editor. Proceedings of the Sixth International Conference on Railway Technology: Research, Development and Maintenance [Internet]. Edinburgh; 2024 [cited 2024 Sep 4]. Available from: https://www.ctresources.info/ccc/paper.html?id=10094

26. Quazi A, Crouch T, Bell J, McGreevy T, Thompson MC, Burton D. A field study on the aerodynamics of freight trains. Journal of Wind Engineering and Industrial Aerodynamics. 2021 Feb 1;209.

27. Quazi A, Crouch T, Bell J, McGreevy T, Thompson MC, Burton D. A field study on the aerodynamics of freight trains with different stacking configurations. Journal of Wind Engineering and Industrial Aerodynamics. 2023 Jan 1;232.

28. Hemida H, Baker C. Large-eddy simulation of the flow around a freight wagon subjected to a crosswind. Comput Fluids. 2010 Dec;39(10):1944–56.

29. Golovanevskiy VA, Chmovzh V V., Girka Y V. On the optimal model configuration for aerodynamic modeling of open cargo railway train. Journal of Wind Engineering and Industrial Aerodynamics. 2012;107–108:131–9.

30. Alam F, Watkins S. Effects of Crosswinds on Double Stacked Container Wagons. In Gold Coast, Australia; 2007.

31. Kocoń A, Flaga A. Critical velocity measurements of freight railway vehicles roll-over in wind tunnel tests as the method to assess their safety at strong cross winds. In: Journal of Wind Engineering and Industrial Aerodynamics. Elsevier B.V.; 2021.

32. Soper D, Baker C, Sterling M. An experimental investigation to assess the influence of container loading configuration on the effects of a crosswind on a container freight train. Journal of Wind Engineering and Industrial Aerodynamics. 2015;145:304–17.

33. Iliadis P, Hemida H, Soper D, Baker C. Numerical simulations of the separated flow around a freight train passing through a tunnel using the sliding mesh technique. Proc Inst Mech Eng F J Rail Rapid Transit. 2020 Jul 1;234(6):638–54.

34. Iliadis P, Soper D, Baker C, Hemida H. Experimental investigation of the aerodynamics of a freight train passing through a tunnel using a moving model. Proc Inst Mech Eng F J Rail Rapid Transit. 2019 Sep 1;233(8):857–68.

35. Bell James R, Burton D, Thompson MC. The boundary-layer characteristics and unsteady flow topology of full-scale operational inter-modal freight trains. Journal of Wind Engineering and Industrial Aerodynamics. 2020 Jun 1;201.

36. Flynn D, Hemida H, Soper D, Baker C. Detached-eddy simulation of the slipstream of an operational freight train. Journal of Wind Engineering and Industrial Aerodynamics. 2014;132:1–12.

37. Soper D. The aerodynamics of a container freight train [PhD Thesis]. University of Birmingham; 2014.

38. Buhr A, Siegel L, Bell J, Henning A. Energy Savings for Freight Trains with Aerodynamically Optimized Loading Schemes. In: Pombo J, editor. Proceedings of the Sixth International Conference on Railway Technology: Research, Development and Maintenance. Edinburgh: Civil-Comp Press; 2024.

39. Soper D, Baker C, Sterling M. Experimental investigation of the slipstream development around a container freight train using a moving model facility. Journal of Wind Engineering and Industrial Aerodynamics. 2014 Dec 1;135:105–17.

40. Lukaszewicz P. Running resistance - Results and analysis of full-scale tests with passenger and freight trains in Sweden. Proc Inst Mech Eng F J Rail Rapid Transit. 2007;221(2):183–93.

41. Wang S, Bell JR, Burton D, Herbst AH, Sheridan J, Thompson MC. The performance of different turbulence models (URANS, SAS and DES) for predicting high-speed train slipstream. Journal of Wind Engineering and Industrial Aerodynamics. 2017 Jun 1;165:46–57.

42. Nayeri CN, Tschepe J, Schulze H, Schell H. Aerodynamic Drag Reduction of Railroad Tank Wagons. Fluids. 2022 Aug 1;7(8).

43. Watkins S, Saunders JW, Kumar H. Aerodynamic drag reduction of goods trains. Vol. 40, Journal of Wind Engineering and Industrial Aerodynamics. 1992.

44. Maleki S. Numerical Investigations into the Aerodynamics of Freight Trains. Monash University; 2019.

45. Lai YC, Barkan CPL, Önal H. Optimizing the aerodynamic efficiency of intermodal freight trains. Transp Res E Logist Transp Rev. 2008;44(5):820–34.

46. Lai YC, L Barkan CP. Options for Improving the Energy Efficiency of Intermodal Freight Trains. Transportation Research Record: Journal of the Transportation Research Board. 2005;47–55.

47. Beagles AE, Fletcher DI. The aerodynamics of freight: Approaches to save fuel by optimising the utilisation of container trains. Proc Inst Mech Eng F J Rail Rapid Transit. 2013 Nov;227(6):635–43.

48. Rochard BP, Schmid F. A review of methods to measure and calculate train resistances. In: Proceedings of the Institution of Mechanical Engineers. 2000. p. 185–99.

49. Somaschini C, Rocchi D, Tomasini G, Schito P. Simplified Estimation of Train Resistance Parameters - Full Scale Experimental Tests and Analysis. In: Proceedings of the Third International Conference on Railway Technology: Research, Development and Maintenance. 2016.

50. Engdahl R, Gielow RL, Paul JC. Train resistance - aerodynamics:Volume 1 of 2. Intermodal car application. In: Railroad energy technology conference. Atlanta; 1987.

51. Maleki S, Burton D, Thompson MC. On the flow past and forces on double-stacked wagons within a freight train under cross-wind. Journal of Wind Engineering and Industrial Aerodynamics. 2020 Nov 1;206.

52. Dirsh WF. Train Energy Model Version 2.0 Technical Manual. In: Publication SD-040. Association of Americal Railroads (AAR); 1992.

53. Arsene S, Spiroiu MA. Study of the Aerodynamics of Freight Trains used in Container Transport. Applied Mathematics, Mechanics and Engineering. 2024 Apr;67(2):787–96.

54. Xu L. A Second Generation URANS Approach for Application to Aerodynamic Design and Optimization in the Automotive Industry. Vol. 14. Massachussets Institute of Technology; 2020.

55. Liang G, Liu T, Xia Y, Chen Z, Dong X, Chen X. Application of periodic boundaries in freight train aerodynamic performance simulations. Alexandria Engineering Journal. 2023 May 1;70:315–29.

56. Strelets M, Allmaras S. Comments on the Feasibility of LES for Wings, and on a Hybrid RANS/LES Approach [Internet]. 1997. Available from: https://www.researchgate.net/publication/236888805

57. Spalart PR, Deck S, Shur ML, Squires KD, Strelets MK, Travin A. A new version of detached-eddy simulation, resistant to ambiguous grid densities. Theor Comput Fluid Dyn. 2006 Jul;20(3):181–95.

58. Cross D, Hughes B, Ingham D, Ma L. A validated numerical investigation of the effects of high blockage ratio and train and tunnel length upon underground railway aerodynamics. Journal of Wind Engineering and Industrial Aerodynamics. 2015 Nov 1;146:195–206.

59. Vardy AE, Reinke P. Estimation of train resistance coefficients in tunnels from measurements during routine operation. In: Proceedings of the Institution of Mechanical Engineers, Part F: Journal of Rail and Rapid Transit. SAGE Pubbications; 1999. p. 71–87.

60. Mei Y. A Generalized Numerical Simulation Method for Pressure Waves Generated by High-Speed Trains Passing through Tunnels. Advances in Structural Engineering. 2013;16(8):1427–36.

61. Liu Z, Soper D, Hemida H, Chen B. A study of the influence of separation bubbles around a generic freight train on pressure waves inside tunnels using 1D and 3D numerical methods. Journal of Wind Engineering and Industrial Aerodynamics. 2023 Sep 1;240.

62. Gawthorpe RG. Wind effects on ground transportation. Journal of Wind Engineering and Industrial Aerodynamics. 1994 May 26;52(1):73–92.

63. Dorigatti F. Rail Vehicles in Crosswinds: Analysis of Steady and Unsteady Aerodynamic Effects through Static and Moving Model Tests. [Birmingham]: University of Birmingham; 2013.

64. Giappino S, Rocchi D, Schito P, Tomasini G. Cross wind and rollover risk on lightweight railway vehicles. Journal of Wind Engineering and Industrial Aerodynamics. 2016 Jun 1;153:106–12.

65. Dorigatti F, Sterling M, Baker CJ, Quinn AD. Crosswind effects on the stability of a model passenger train-A comparison of static and moving experiments. Journal of Wind Engineering and Industrial Aerodynamics. 2015 Mar 1;138:36–51.

66. Noguchi Y, Suzuki M, Baker C, Nakade K. Numerical and experimental study on the aerodynamic force coefficients of railway vehicles on an embankment in crosswind. Journal of Wind Engineering and Industrial Aerodynamics. 2019 Jan 1;184:90–105.

67. Premoli A, Rocchi D, Schito P, Tomasini G. Comparison between steady and moving railway vehicles subjected to crosswind by CFD analysis. Journal of Wind Engineering and Industrial Aerodynamics. 2016 Sep 1;156:29–40.

68. Xie Y, Wu Z. Simulation Research on Aerodynamic of Railway Freight Train Based on CFD Method. In: Advances in Transdisciplinary Engineering. IOS Press BV; 2022. p. 433–41.

69. Liu Y, Hemida H, Liu Z. Large eddy simulation of the flow around a train passing a stationary freight wagon. Proc Inst Mech Eng F J Rail Rapid Transit. 2014;228(5):535–45.

70. Gallagher M, Morden J, Baker C, Soper D, Quinn A, Hemida H, et al. Trains in crosswinds – Comparison of full-scale on-train measurements, physical model tests and CFD calculations. Journal of Wind Engineering and Industrial Aerodynamics. 2018 Apr 1;175:428–44.

71. Li R, Soper D, Xu J, Jia Y, Niu J, Hemida H. A Separated-Flow Model for 2-D Viscous Flows around Bluff Bodies Using the Panel Method. Applied Sciences (Switzerland). 2022 Oct 1;12(19).

72. Bocciolone M, Cheli F, Corradi R, Muggiasca S, Tomasini G. Crosswind action on rail vehicles: Wind tunnel experimental analyses. Journal of Wind Engineering and Industrial Aerodynamics. 2008 May;96(5):584–610.

73. Gil N, Baker CJ, Roberts C. The measurement of train slipstream characteristics using a rotating rail rig. In: BBAA VI International Colloquium on: Bluff Bodies Aerodynamics & Applications. Milano; 2008.

74. Bell JR, Burton D, Thompson MC, Herbst AH, Sheridan J. Flow topology and unsteady features of the wake of a generic high-speed train. J Fluids Struct. 2016 Feb 1;61:168–83.

75. Bell James, Buhr Alexander, Henning Arne. Measuring the Oncoming Flow that Operational Freight-Trains Experience Using the DLR FR8-LAB. In: New Results in Numerical and Experimental Fluid Mechanics XIV. Springler; 2023.

76. Soper D, Baker C. A full-scale experimental investigation of passenger and freight train aerodynamics. Proc Inst Mech Eng F J Rail Rapid Transit. 2020 May 1;234(5):482–97.

77. Negri S, Tomasini G, Schito P, Rocchi D. Full scale experimental tests to evaluate the train slipstream in tunnels. Journal of Wind Engineering and Industrial Aerodynamics. 2023 Sep 1;240.

78. Soper D, Gallagher M, Baker C, Quinn A. A model-scale study to assess the influence of ground geometries on aerodynamic flow development around a train. Proc Inst Mech Eng F J Rail Rapid Transit. 2017 Sep 1;231(8):916–33.

79. Bell J, Buhr A, Siegel L, Volkert R, Michael O, Renschler C, et al. The Effect of Loading Configuration on the Slipstream of Freight Trains. In: Proceedings of the Sixth International Conference on Railway Technology: Research, Development and Maintenance. Civil-Comp Press; 2024. p. 1–14.

80. Baker CJ, Dalley SJ, Johnson T, Quinn A, Wright NG. The slipstream and wake of a high-speed train. In: Proceedings of the Institution of Mechanical Engineers, Part F. SAGE Publications; 2001. p. 83–99.

81. Soper D, Jesson M, Baker C. Assessing aerodynamic risk to enable freight speeds above 75 mph. 2025 May.

82. Soper D, Baker C. "Superfast freight": aerodynamic assessments and mitigations Technical report T1303. 2023 May.

83. Paz C, Suárez E, Gil C, Cabarcos A. Effect of realistic ballasted track in the underbody flow of a high-speed train via CFD simulations. Journal of Wind Engineering and Industrial Aerodynamics. 2019 Jan 1;184:1–9.

84. Heft AI, Indinger T, Adams NA. Introduction of a New Realistic Generic Car Model for Aerodynamic Investigations. In 2012.

85. Zhang Y, Wang D. Numerical Analysis of the Aerodynamic Characteristics of the Open Line Intersection of Fast Freight Train with the Speed of 160 km/h. In: Journal of Physics: Conference Series. IOP Publishing Ltd; 2021.

86. Soper D, Baker C, Jackson A, Milne DR, Le Pen L, Watson G, et al. Full scale measurements of train underbody flows and track forces. Journal of Wind Engineering and Industrial Aerodynamics. 2017 Oct 1;169:251–64.

87. Soper D, Flynn D, Baker C, Jackson A, Hemida H. A comparative study of methods to simulate aerodynamic flow beneath a high-speed train. Proc Inst Mech Eng F J Rail Rapid Transit. 2018 May 1;232(5):1464–82.

88. Paz C, Suárez E, Gil C. Numerical methodology for evaluating the effect of sleepers in the underbody flow of a high-speed train. Journal of Wind Engineering and Industrial Aerodynamics. 2017 Aug 1;167:140–7.

89. Corniani L, Schito P, Bruni S. Aerodynamics of Freight Trains: An Open Database of Geometries for CFD Analyses. In: Pombo J, editor. Proceedings of the Sixth International Conference on Railway Technology: Research, Development and Maintenance [Internet]. Edinburgh: Civil-Comp Press; 2024. Available from: http://www.ctresources.info/ccc/paper.html?id=10113

90. Roache PJ. QUANTIFICATION OF UNCERTAINTY IN COMPUTATIONAL FLUID DYNAMICS. Vol. 29, Annu. Rev. Fluid. Mech. 1997.

91. Celik IB, Ghia U, Roache PJ, Freitas C. Journal of Fluids Engineering Editorial Policy Statement on the Control of Numerical Accuracy.

92. Andersson E, Häggström J, Sima M, Stichel S. Assessment of train-overturning risk due to strong cross-winds. Proc Inst Mech Eng F J Rail Rapid Transit. 2004 May 1;18:213–23.

93. di Gialleonardo E, Melzi S, Tomasini GM. Crosswind effect on “high-speed” freight wagons. In: Proceedings of the 14th International Conference on Vehicle System Dynamics, Identification and Anomalies [Internet]. 2014 [cited 2025 Jul 16]. p. 173–83. Available from: https://www.scopus.com/pages/publications/84987973936

Appendix C: paper “Aerodynamics of Freight Trains: addressing the complexity of train geometry through an open database”

This paper is ready for submission and will be submitted not later than September 10th 2025 for a special issue of the international journal “Promet - Traffic & Transportation Journal”.

In the following pages, the final draft of the manuscript ready for submission is reported.

Aerodynamics of Freight Trains: addressing the complexity of train geometry through an open database

L. Corniani[1*], Paolo Schito1, James Bell[2], Joao Pombo[3], Stefano Bruni[1]
1 Dipartimento di Meccanica, Politecnico di Milano, Italy
2 Institute of Aerodynamics and Flow Technology, German Aerospace Center (DLR), Göttingen, Germany
3 Institute of Railway Research, University of Huddersfield, UK
*corresponding author luca.corniani@polimi.it

Abstract

The study of the aerodynamics of freight trains is important for managing the aerodynamic phenomena that take place while operating freight trains, especially the aerodynamic drag.
Computational Fluid Dynamics (CFD) is often use for investigation of these flows. The majority of the studies made in this field, have regarded container wagons, but many more wagon types are used in the industry.
To address the need for efficient production of these geometries, a database of representative wagon and locomotive geometries is needed (similarly to what has been done with the DrivAer project in the automotive industry)
In this work, the production and characteristics of this database are presented, and some simulation results with the database geometries are reported and discussed to showcase their use.

Keywords: train aerodynamics, freight trains, database, container, CFD, URANS

1 Introduction

In its white paper (REF), the European Union outlines its goals to for shifting the transport of freight from road to rail of waterways (both responsible for less CO_2 emissions for each tkm than trucks (REF)). The pursuit of this goal entails the eventual increase in the speed of freight trains to at least 160 km/h (Geischberger et al. [1]).

Aerodynamic forces grow approximately with the square of the velocity of the flow, thus increasing the train speed results in greater aerodynamic forces on the vehicle. At current freight trains speeds, aerodynamic forces can already contribute for the majority of the overall resistance to forward motion (REF), at 160 km/h they would be paramount.

Research from Quazi et al. [2] and Alam et al. [3] shows that freight trains encounter wind from yaw angles mostly below 20° (this would be even more true at higher speeds), and therefore the main component of the aerodynamic force on a moving train is drag. This means that the increase of service speed has direct consequences for the cost and environmental impact of the operation of the train, since the mechanical power spent by the locomotive is proportional to the overall resistance to motion. Other components of the force are also of interest, since both lift and side force generate overturning moment on the wagons and must be contained to reduce the risk of derailment.

A subject of intense study directly linked to drag is the effect of empty wagons and of the size of gaps between containers, Maleki et al. [4] showed that the pressure component of drag is closely related to the size of the gap between containers.

Slipstream is also linked to drag, because a greater transfer of momentum to the surrounding air by the vehicle will generate stronger winds in the air surrounding it. Thus, like with drag, slipstream velocities generated by a freight train tend to increase for larger gaps (Flynn et al. [5] and Li et al. [6]).I In the absence of crosswind, these velocities are not sufficient to put a person stability at risk, but crosswind amplifies this effect enough to destabilize large portions of the population (Flynn et al. [7]).

Unlike streamlined passenger trains, freight trains behave as bluff-bodies and thus the flow around these vehicles is more turbulent and intrinsically unsteady. The study of freight train aerodynamics is further complicated by the fact that they can be composed of a variety of wagons with diverse geometries. These differences between passenger and freight trains call for an investigation of the flow around the latter as a separate endeavour.

The aerodynamics of freight train has been studied in the literature with both numerical and experimental methods. Experimental methods measure actual physical properties of the flow, and thus are often considered more realistic, however different sources of error exist such as the error of the measurement instruments.

Most experimental studies on freight trains are conducted in wind tunnels. Alam et al. [8] performed a wind tunnel test on a 1:15 model scale of a double stacked container wagon in isolation. Subsequent studies by Giappino et al. [9] (AGGIUNGI a study of slipstream… DEL 2008), Kocon et al. [10] and Alam et al. [3] focused on the risk of overturning caused by crosswind on freight trains at different yaw angles and gap sizes. Wind tunnel tests have also been used by Soper et al. [11] and Sterling et al. [12] to study the slipstream velocities generated by freight trains and found them to be much greater than what was observed in passenger trains.

In all wind tunnel experiments that involve freight trains, the Reynolds number of the test is much lower than in full-scale experiments and this makes the latter more reliable, however the former is still often preferred for the lower costs. The independence of the flow from Reynolds number for values of Reynolds number greater than $2.5 \cdot 10^5$ has been established in different works (e.g. Bocciolone et al. [15]). Soper et al. [16] used full-scale experiments to compare the aerodynamics of passenger and freight trains and found that freight trains at low speed generate slipstream velocities higher than the passenger trains (although not in violation of the TSI regulations). The measurement of a full-scale underbody flow has been used by Soper et al. [17] to conclude that on well-maintained tracks the aerodynamic forces on ballast and the inertial ones due to track displacement are comparable, but poorly maintained tracks may increase the risk of ballast flight significantly.

Numerical studies allow to evaluate the flow in every point of the domain; however, the results are also affected by different sources of error, such as the physical modelling of the problem.

One of the most significant decisions to make in CFD is the modelling method for turbulence. Different works have been published comparing the accuracy and cost of different methods (Wang et al. [18], Wang et al. [19] and Maleki et al. [20]) and they agree on the fact that RANS is unsuitable for the simulation of freight trains because of the pronounced unsteadiness of the flow. The expensive LES (or more often in recent works ELES, DES or DDES) are generally agreed to be the most accurate methods, predicting flow topology and aerodynamic coefficients in line with experimental results. URANS has shown an intermediate level of accuracy between RANS and LES. It should be noted however, that while RANS methods fail to predict the numerical value of aerodynamic coefficients, they predict their trends and are suitable for comparing the performance of different geometries (Maleki et al. [20]). This last consideration is particularly important for the industrial sector, where RANS and URANS methods are still preferred despite their limitations. This is of course because of the limited availability of computational power that make the LES variants unfeasible for the industry.

The Academics4Rail research project, funded by the European community under the Europe's Rail funding programme, has launched a comprehensive investigation on the aerodynamics of freight trains. The objective is to define guidelines for the creation of CFD models of freight trains, analyse different realistic operation scenarios and synthesise the results in guidelines for safer and more efficient operation of freight trains in regard of aerodynamic effects.

Given the breadth of the problems addressed, the need for the efficient definition of geometric models for single vehicles (locomotives and wagons) and for complete freight trains becomes apparent. Therefore, a first part of the research is devoted to creating a database of geometries for vehicles and vehicle parts in formats that are compatible with software for CFD simulation. In this way, complex geometries representative of realistic freight operation scenarios can be efficiently created. In the creation of the database, vehicle geometries are designed with different levels of detail, allowing the efficient creation of simpler and more detailed CFD models, in view of finding a trade-off between accuracy and computational efficiency.

This paper presents the database already exposed at the RAILWAYS 2024 conference (REF) and further shows a case use with geometries representative of a typical container train with the lowest and highest level of detail.

The paper is structured as follows: in section 2 of the paper a detailed description of the geometries and the process by which they have been created and stored in the database is provided. In section 3 an exemplary CFD analysis is presented, analysing the mesh independence and a comparison between levels of detail. Finally, in section 4 conclusion and final remarks are drawn.

2 The database of freight train geometries

Rephrase, compact the figures

Unlike passenger trains, freight trains exhibit a wide variety of geometries both because of different wagons that make them up and because of the many different compositions (what type of wagons they are made of, and in what order) that they can have.

The study of the aerodynamics around these vehicles therefore is only possible if an efficient and versatile method for producing diverse freight train geometries is developed. The aim of the proposed database is to address this need while allowing the user to balance between higher levels of detail and computational cost.

In order to organize and navigate the database, a categorization of freight wagons needed to be chosen. While no official classification exists, freight wagons can be broadly distinguished according to these categories: Open wagons, Covered wagons, Flat wagons, Dump cars, High-capacity wagons, Special wagons, and Tank wagons. This way of distinguishing freight wagons has been also adopted with minor variations elsewhere in literature, however, these specific categories have been taken from Principe [21]. Locomotives are more homogenous in their geometry, so they have not been classified in a similar way, instead three versions meant to resemble slight variations in existing locomotives are proposed.

All wagons are composed of three parts: a wagon plane, bogies, and cargo (where cargo refers to the geometry above the wagon plane). In Figure 8, the components of the dumpcar wagon (on the right) and the components of the B version of the locomotive (on the left) are shown.

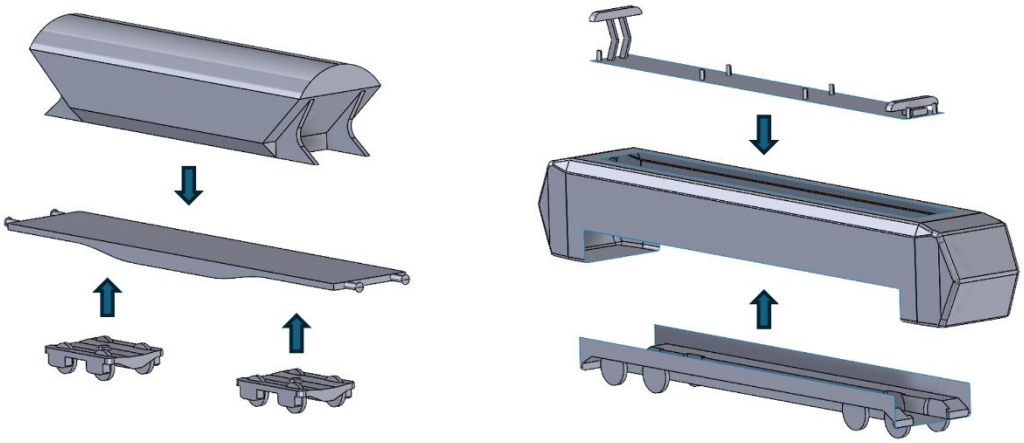

Figure 8, components assembly of wagons (left) and locomotives (right)

The advantage of the modular approach is three-fold: it allows the user to select different levels of details for parts of the vehicles, it allows the possiblity of better comparisons between various cases, and finally, it allows for faster production and update of geometries.

The database, as presented at the RAILWAYS 2024 conference in Prague (REF) includes geometries of both locomotives and wagons. The locomotives are made of three parts: the main body, the underbody, and the roof. What differentiates one locomotive version from another is the main body, since the underbody and roof are designed so as to be interchangeable.

The design of the main bodies for all locomotive versions followed the same workflow: first, a basic structure is defined through the use of a certain number of parameters as shown in **Errore. L'origine riferimento non è stata trovata.**, then the volume enclosed in the structure is extruded and the edges are rounded (with the radii being parametrically defined as well), and finally, the surface of the main body is obtained from the volume.
After the modelling of the geometry of the main bodies of the locomotives, the surfaces were trimmed along well-defined curves. The final result is an open surface with boundaries that match those of other components of the locomotive, so that when they are all assembled, they constitute a closed surface again.

Roof and underbody geometries in real locomotives are very different from model to model, , however, some parts of these geometries are standardized. Pantographs have been modelled to resemble the actual dimensions reported by Baker et al. [22]. Figure 9 (on top) shows the roof geometries, from left to right in increasing level of detail.

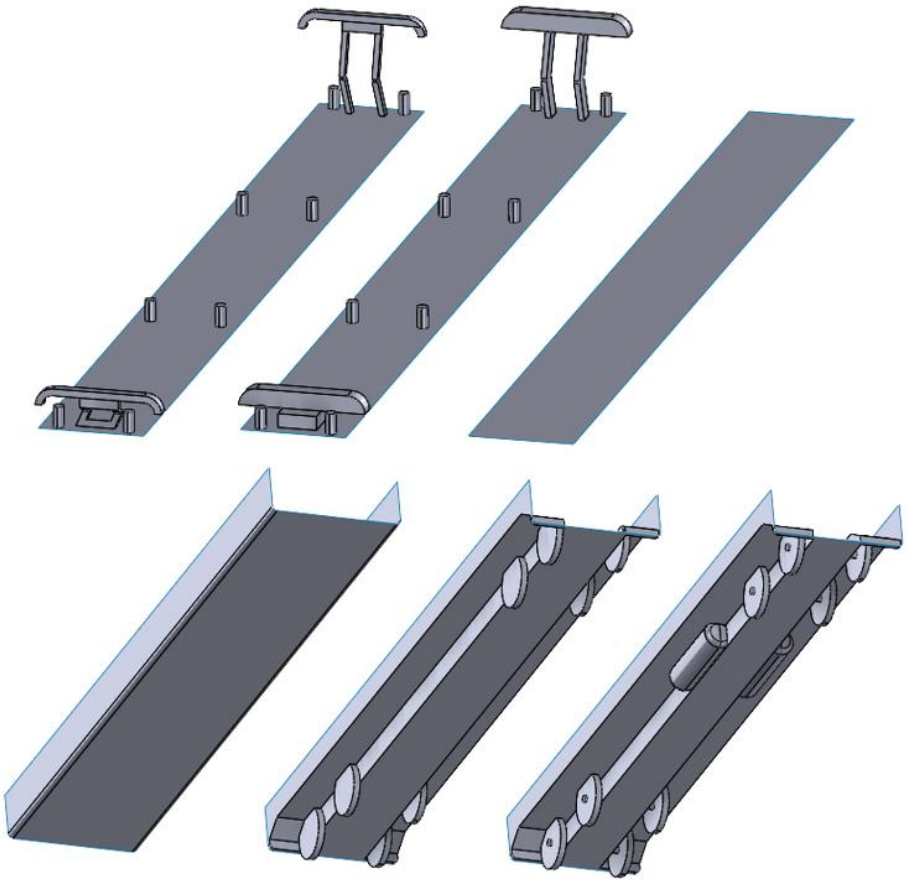

Figure 9: Roof components and underbody components in different levels of detail.

The final component of the locomotive geometry is the underbody (shown in Figure 9 at the bottom). Similarly to the roof, the underbody geometries of actual locomotives are very diverse, and so the same strategy has been adopted; the dimensions of standardized parts have been taken from Principe [21] to make the geometry broadly realistic. Figure 10 shows the complete (assembled) locomotive geometry.

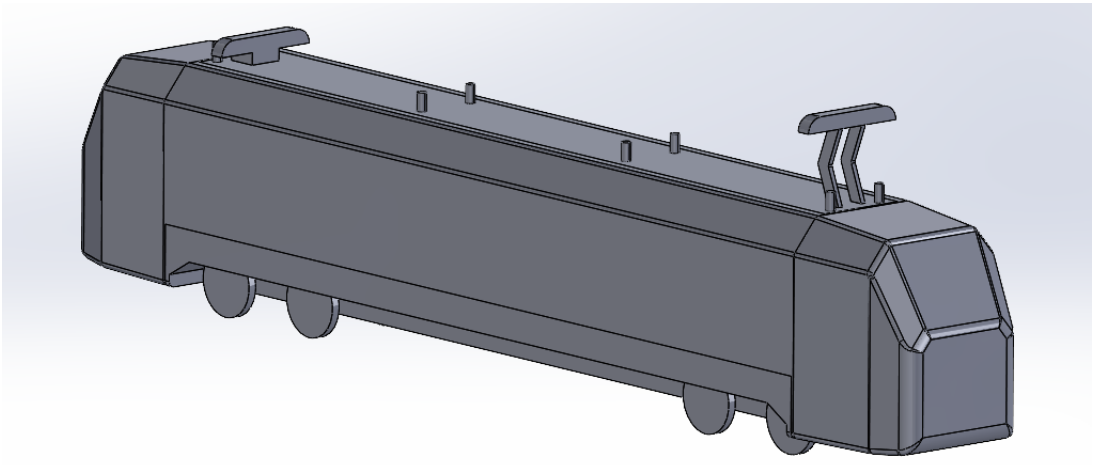

Figure 10: Assembled locomotive, version C, medium level of detail.

Like for other parts, the geometries of the roof and underbody have been made available in different levels of detail. The process of removing details from the geometries is referred to as defeaturing. When designing a vehicle geometry for CFD, all details have some effect on the flow, however some may well be negligible depending on the objective of the simulation. Therefore, a balance needs to be struck between computational cost and accuracy.

Experimental and numerical work is being undertaken to assess the effects of greater level of geometrical detail for the measurement of drag in freight trains, for the present work the following general rule has been employed: features that changed the front area of the geometry were deemed more impactful on the flow than features that did not, so the former were removed only in the last iterations of defeaturing, and the latter were removed immediately. Similarly, the more voluminous features were deemed more impactful on the flow than smaller ones.

As shown in Figure 8, all wagons are composed of three components, of which two are the same for all wagon types. It should be noticed that not all wagon types have a cargo, indeed flat wagons may carry one container, two container, or be empty, in the latter case the wagon is composed by plane and bogies alone.

All wagon components have been designed as closed surfaces and feature planar faces that act as interface between components. This means that all components at all levels of detail must be present planar surfaces in the right places to allow for the faces to overlap in one interface.

Figure 11 shows in red the interfaces between bogies and plane and in green the one between plane and cargo.

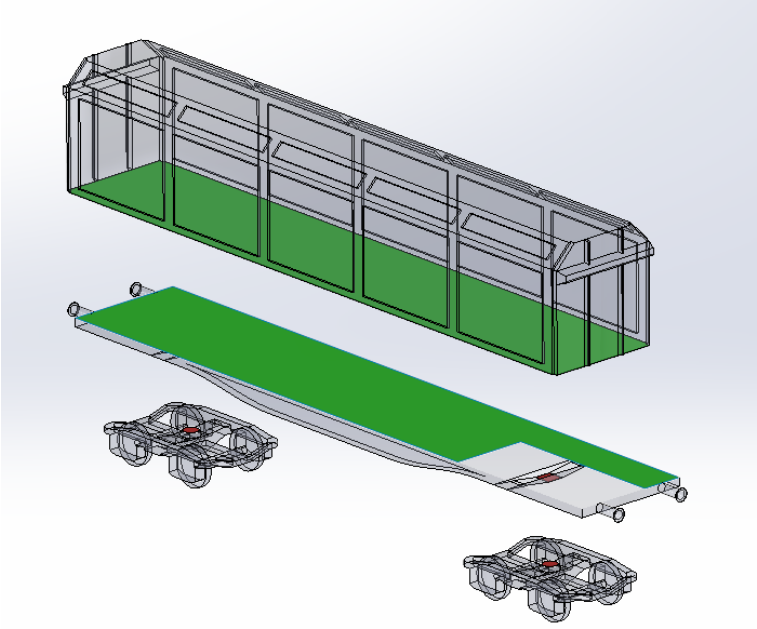

Figure 11: Components of a covered wagon with its interface surfaces highlighted.

The geometries in the database have been designed to be realistic, but do not replicate any existing rail vehicle, with the exception of the bogies. The bogies geometries, in its highest level of detail, accurately replicates the geometry of the Y25 bogies. Figure 13 shows the bogies and the wagon planes in three levels of detail.

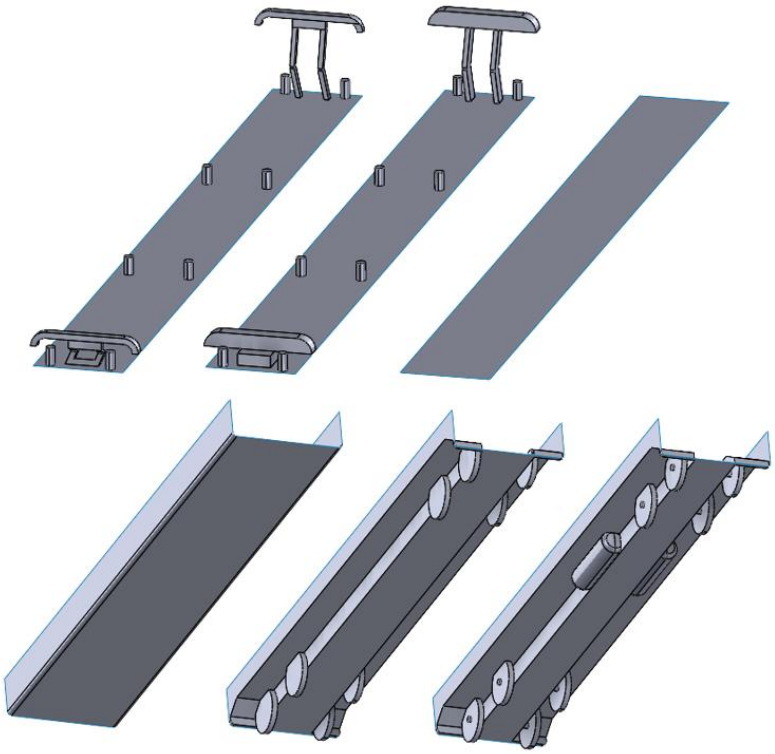

Figure 12, roof components in different levels of detail (top) and underbody comopnents in different levels of deatil (bottom)

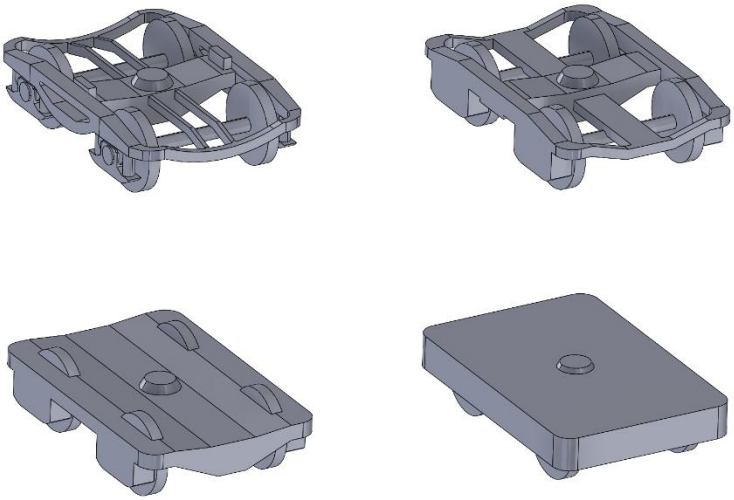

Figure 13, Y25 bogies modeles in different levels of detail

All the geometries showcased in this work have been made available in STEP format in a public GitHub repository. Preassembled full wagon with consistent levels of detail among the components have been prepared and uploaded, as well as the single components in all levels of detail.

The database presented thus far is a useful starting point for the study of aerodynamics around different freight trains, including all the most used types of wagons, however, further improvements have been made since its first presentation at the RAILWAYS 2024 conference. More geometries of tanks (and their surrounding frames) have been added to the database together with model-scale CAD files for use in model-scale experiments (both with force scale and pressure taps).

Further additions are still possible (e.g. double stacked containers, longer versions of covered and flat wagons). Another way of improving on the present work would be to simplify the process of composing a train of chosen composition, a software to manipulate the coordinates within the files would be the most suitable tool for this.

3 CFD use cases: single wagon

In this section, some use cases of some of the database geometries will be provided. First, the simple case of a single container wagon with a 40 ft container moving at 160 kmh^{-1} in steady air is considered, secondly, a train of one locomotive and two wagons will be considered. In the latter case, the first wagon behind the locomotive will be composed of a less-detailed flat wagon and container, to compare the results with the single wagon.

The simulations on the single wagons have been carried out using the open-source software OpenFoam v10.In order to reduce computational time, a first steady simulation was run to allow the develop a wake. This flow solution was not realistic, given that the transient nature of the actual flow, but it was more similar to a realistic flow than the the potential flow solution (which instead was the starting condition for the steady simulation). The steady state simulation was carried out with the SIMPLE algorithm using the linear scheme for the gradient of velocity and the upwind scheme for its divergence.

Starting from the solution of the steady solver, the unsteady simulation was run with the k-ω SST turbulence model (the same model was adopted for both steady-state and transient runs). The unsteady simulations were carried out with the PIMPLE algorithm, with the same settings as before (except of course for the time-derivative, for which the implicit Euler scheme was chosen).

Figure 14 shows the domain dimensions in terms of lengths (L), widths (W) and heights (H) of the wagon.For the ground and the wagon patches, a zero-gradient boundary condition was chosen for pressure and a no-slip condition for the velocity. The inlet velocity was set to 160 kmh^{-1} and at the outlet pressure a zero-gradient was imposed. Zero-gradient for pressure and slip condition for velocity were set on all remaining patches.

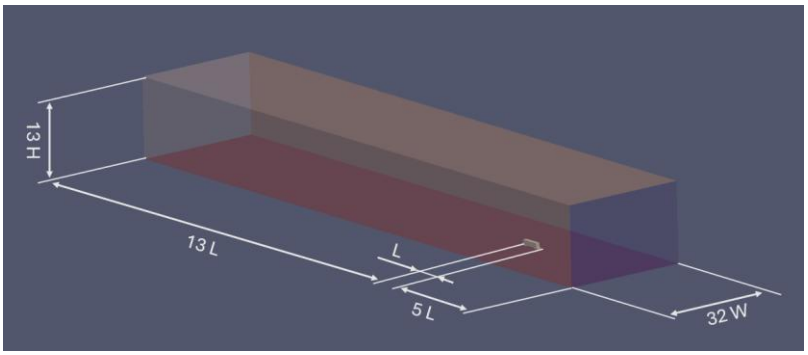

Figure 14: Simulation domain.

The meshes were all structured and have been obtained with the inbuilt OpenFoam application snappyHexMesh, with a refined region around the wagon.

A convergence study was carried out on the single wagons (the same settings and refinement level will be deemed adequate for the multiple-wagons simulations). Table 3 reports the aerodynamic coefficients for lift and drag determined with meshes of different level of refinement in a steady-state simulations. The coefficients have been calculated using a reference area of 10 m^2 according to expressions (1).

$$C_D = \frac{2D}{\rho A {U_f}^2} \qquad C_L = \frac{2L}{\rho A {U_f}^2} \qquad C_S = \frac{2S}{\rho A {U_f}^2} \qquad (1)$$

Where D is the pressure drag, L is the pressure lift, S is the pressure side force, ρ is the density of the air, A is the reference area and U_f is the freestream velocity of the air (44.44 ms^{-1})
Table 3 shows the force coefficients for drag and lift on the single wagon. As can be observed, the coefficients show remarkable convergence despite the stationary solver. It can be noticed that the variations of aerodynamic coefficients remain below 1% beyond the 11.9 million cells grid, thus the results are deemed to be mesh independent beyond this level of refinement. It will be assumed in this work that this level of refinement is suitable for the unsteady solver as well.
. The convergence of the force coefficients to a given value is not sufficient to infer the accuracy of that value, indeed, because the flow around freight wagons is strongly unsteady it should be expected that the steady-state solver will not be able to accurately predict the value of the aerodynamic forces. This is a well know limitation of the RANS method that has been demonstrated before by Maleki et al. [20].In the same work however, it is shown that the RANS method remains capable of predicting trends in aerodynamic forces (although the values of the forces are not accurate) and is useful for comparative investigations.

Number of cells [millions]	C_D [-]	C_L [-]	$\Delta C_D/C_D$ [%]	$\Delta C_L/C_L$ [%]
2.9	0.809	-0.207	+0.24%	-6.94%
4.4	0.811	-0.192	+0.44%	+5.84%
6.3	0.814	-0.204	+0.65%	+8.04%
8.9	0.819	-0.220	-0.06%	+1.08%
11.9	0.819	-0.222	-0.53%	-0.63%
15.6	0.815	-0.221	+0.59%	-0.44%
20.1	0.819	-0.220		

Table *3*: Convergence of aerodynamic coefficients for with different grids

The URANS method, is more capable of capturing the unsteady nature of the flow and therefore is more suitable for the simulations of flows around bluff bodies such as this container wagon. The greater accuracy of the URANS method with respect to steady RANS has been shown in the literature before (altough they share similar limitations in the prediction of the flow topology, see Wang et al. [18] and Maleki et al. [20]).

In Table *4* the results of the URANS runs on a sinlge wagon with two levels of detail are shown. These results show a significant improvement in accuracy with respect to the RANS method, and in fact are comparable to results in the literature obtained with much more accurate methods (see for example Östh et al. [23] who obtained a drag coefficient value of 0.90).
Finally, Figure 15**Errore. L'origine riferimento non è stata trovata.** shows the magnitude velocity field on the xz-plane and the longitudinal velocity profiles on top of the container in correspondence to the white lines, which demonstrate that the simulation captured the recirculation of the flow.

	C_D [-]	C_L [-]	C_S [-]
Less detailed wagon	0.862	-0.218	0.011
Medium detailed wagon	0.878	-0.170	0.006

Table *4*: Time-averaged aerodynamic coefficients from unsteady, single-vehicle simulations.

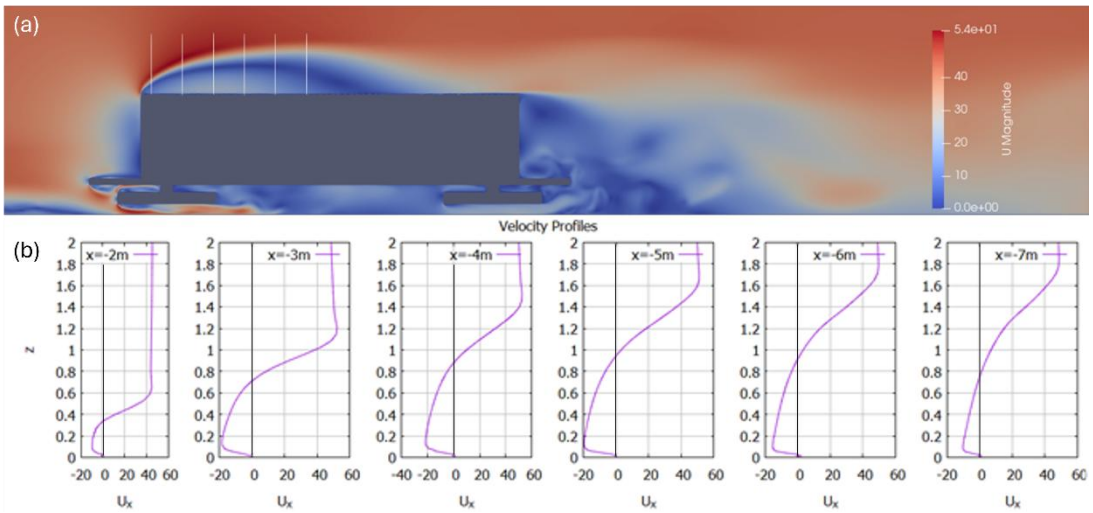

Figure 15, (a) Magnitude velocity field of the unsteady simulation, (b) Longitudinal velocity profile within recirculation bubble

4 CFD use cases: multiple wagons

After the single-wagon simulation, multiple-wagons use case is presented. In this simulation, a train composition of three vehicles is used: a locomotive followed by two wagons, as shown in Figure 16.

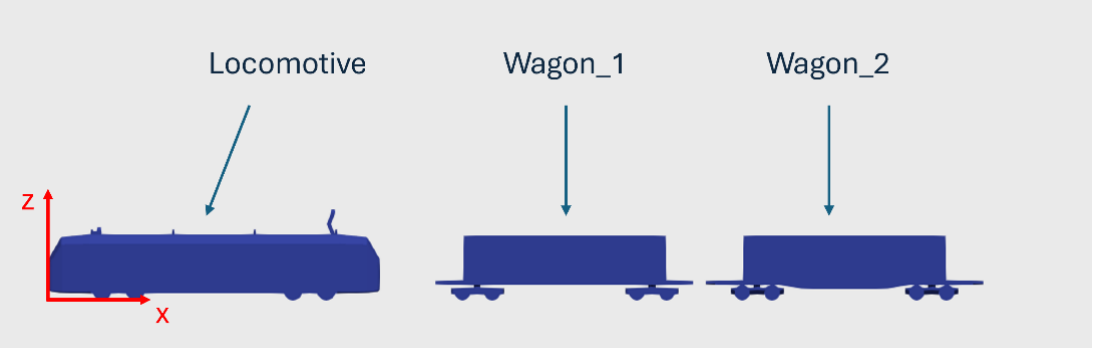

Figure 16, Train composition of multi-vehicle simulation

In this simulation the effects of vehicles upstream on the force coefficient will be investigated, with special attention on the trailing wagon.

The first wagon (indicated in Figure 16 as wagon_1) has been composed of the least detailed components, while the trailing wagon (indicated in Figure 16 as wagon_2) has been composed of medium-detailed components. This decision is motivated by the fact the vehicle of interest for this use case is wagon_2, while wagon_1 and the locomotive are useful only for producing a sufficiently realistic wake. This is an example of how the availability of different levels of detail in the geometries could allow the user to customize the setup in order to balance the computational cost and accuracy of the simulation.

The locomotive used is the version C, while the wagon_1 and wagon_2 are respectively the less detailed version and the medium-detailed version of the flat wagon. The gaps between locomotive and wagon_1 and between wagon_1 and wagon_2 are both approximately 4.8 m in length (equivalent to 2 times the wagon width).

The mesh used for this simulation was constructed with the same level of refinement as the one deemed adequate for the previous case, while the settings of the solver were left unchanged.

The aerodynamic force coefficients on all the vehicles involved were calculated, and are reported in Table 5

Vehicle	C_D [-]	C_S [-]	C_L [-]
Locomotive	0.450	-0.005	0.025
Wagon_1	0.477	-0.025	0.006
Wagon_2	0.294	0.004	0.0132

Table 5, Aerodynamic force coefficients on vehicles of multi-vehicle simulations

It can be observed in Table 5 that for both wagons, the drag coefficients are lower than the ones obtained in the single-vehicle simulation. This is to be expected because of the effect of the wake caused by upstream vehicles, which slows down the flow and leaves it with less momentum for when it meets the wagons. The first wagon encounters the flow after only the locomotive, and its drag coefficient is reduced by 45% with respect to the same geometry in free flow. The first wagon slows the flow further, causing the drag coefficient to be even smaller in the second wagon. In fact, the drag coefficient of wagon_2 is only 33% of the drag coefficient of the same geometry in free flow.

Particularly bluff bodies like container wagons experience high drag because they slow they tend to carry more air with them as they pass through it. This follows from the conservation of momentum, since the aerodynamic drag experienced by the wagon is equivalent to the rate of momentum transferred by the wagon to the surrounding air.

In Figure 17 the time-averaged total pressure coefficient (C_{pt}) field is shown. This quantity is defined in equation 2 and it quantifies the variation in the total pressure of the flow with respect to the freestream.

$$C_{pt} = \frac{p - p_f + \frac{1}{2}\rho U^2}{p_f + \frac{1}{2}\rho {U_f}^2} \qquad (2)$$

Where p is the static pressure of the flow, p_f is the static pressure of the freestream flow (in the simulation, this quantity was set to zero) and U is the magnitude of the speed of the flow.

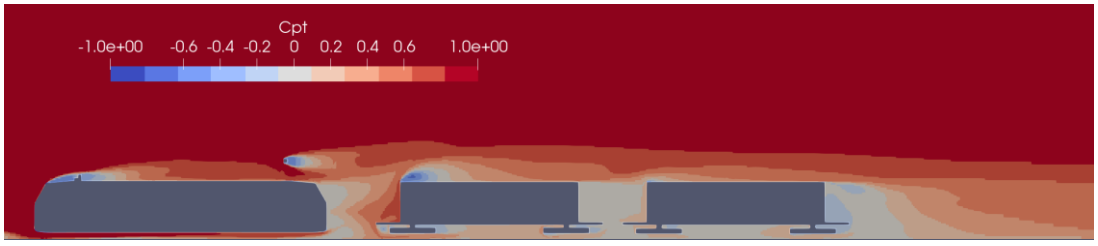

Figure 17, Time-averaged total pressure coefficient field in unsteady multi-vehicle simulation

Observing Figure 17 it is possible to identify the regions of the flow where there are losses of total pressure and thus identify regions of high turbulence. All three vehicles display a flow separation at the upstream top edge, however, the separation is visibly smaller in the downstream wagon that in wagon_1. This is explained by the reduced velocity in the flow.

Figure 18 and Figure 19 show the time-averaged pressure coefficient in the flowfield and on the vehicle surface respectively (see equation 3).

$$C_p = \frac{p - p_f}{\frac{1}{2}\rho {U_f}^2} \quad (2)$$

The Cp coefficients shown in Figure 18 and **Errore. L'origine riferimento non è stata trovata.**Figure 19 are consistent with the diminishing drag coefficient of the wagons. High-pressure regions are present upstream of all vehicles, however, the effect is less pronounced as the vehicle is further from the train nose. Additionally, the last wagon is followed by a low pressure region that increases the drag, while the locomotive and first wagon are not. This occurs because the second wagon is not followed by another vehicle, allowing the wake to develop fully. If more vehicles hade been added, the drag coefficient of the second wagon would have presumably been lower.

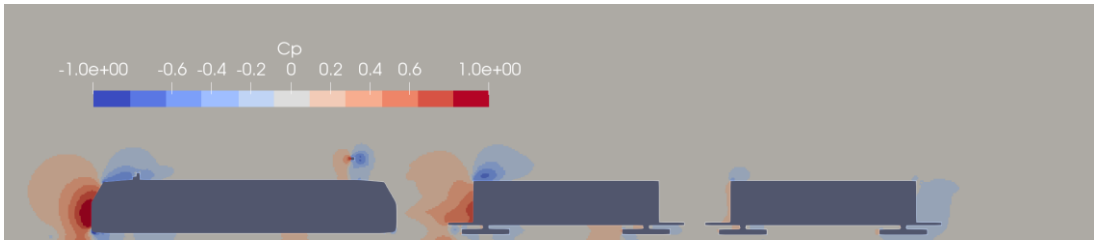

Figure 18, Time-averaged pressure coefficient field in unsteady multi-vehicle simulation

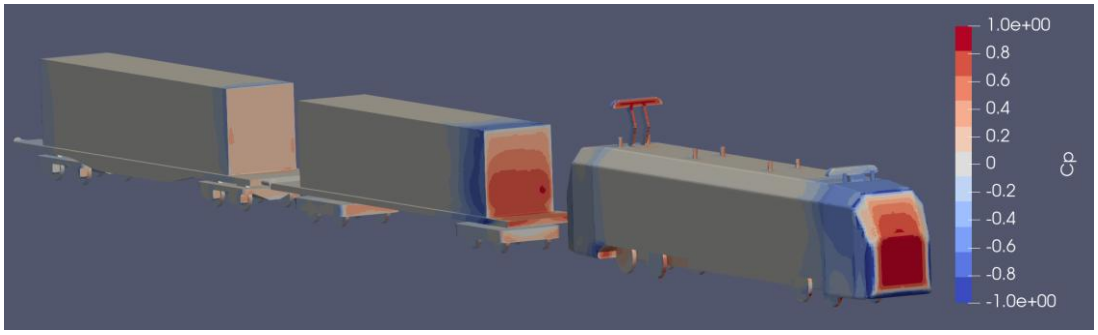

Figure 19, Time-averaged pressure coefficient on the geometry surface in unsteady multi-vehicle simulation

In Figure 19 regions of low pressure are visible immediately downstream of the corners of the front face of each vehicle. These regions show the presence of recirculation bubble that take place where the air flow away from the stagnation region in the front, and causing flow separation at the corners.

5 Conclusions and Contributions

In this work, a database of realistic freight wagons and locomotives geometries has been proposed, with the purpose of offering a quick and efficient way of producing geometries for CFD. The proposed geometries are representative of different realistic vehicles but can also be assembled with custom levels of detail in different parts. Different types of wagons and locomotives are made available in the database, allowing for the simulation of trains that are realistic in composition too (instead of being only composed of container wagons).

In this work, some CFD simulations were also conducted as demonstration of the use of the database. The flow around single wagons has been simulated (with steady and unsteady solvers) and has been compared to the flow around the same geometries in a train. In the multiple-vehicles simulation, a lower level of detail has been chosen for the upstream wagon than the downstream one,

further demonstrating the versatility of the database for the construction of geometries that balance accuracy and computational cost.

Finally, the flow around the vehicles has been shown and discussed, particularly the flow around multiple vehicles. Some of the major structure expected in the flow (e.g. the recirculation regions at the corners of the vehicles or the stagnation regions in front of them) have been identified and the drag coefficients have been found to decrease as the vehicle was placed further from the nose of the train.

Acknowledgements

The research reported in this paper has received funding from the European Union's Horizon Europe research and innovation programme under grant agreement: HORIZON-ER-JU-2022-ExplR-04. Views and opinions expressed are however those of the authors only and do not necessarily reflect those of the European Union or Europe's Rail Joint Undertaking. Neither the European Union nor the granting authority can be held responsible for them.

References

[1] J. Geischberger and M. Moensters, "Impact of faster freight trains on railway capacity and operational quality," *International Journal of Transport Development and Integration*, vol. 4, no. 3, pp. 274–285, Jul. 2020, doi: 10.2495/TDI-V4-N3-274-285.

[2] A. Quazi, T. Crouch, J. Bell, T. McGreevy, M. C. Thompson, and D. Burton, "A field study on the aerodynamics of freight trains with different stacking configurations," *Journal of Wind Engineering and Industrial Aerodynamics*, vol. 232, Jan. 2023, doi: 10.1016/j.jweia.2022.105245.

[3] F. Alam and S. Watkins, "Lateral stability of a double stacked container wagon under crosswind," *Proceedings of the International Conference on Mechanical Engineering 2007*, 2007.

[4] S. Maleki, D. Burton, and M. C. Thompson, "Flow structure between freight train containers with implications for aerodynamic drag," *Journal of Wind Engineering and Industrial Aerodynamics*, vol. 188, pp. 194–206, May 2019, doi: 10.1016/j.jweia.2019.02.007.

[5] D. Flynn, H. Hemida, D. Soper, and C. Baker, "Detached-eddy simulation of the slipstream of an operational freight train," *Journal of Wind Engineering and Industrial Aerodynamics*, vol. 132, pp. 1–12, 2014, doi: 10.1016/j.jweia.2014.06.016.

[6] C. Li, D. Burton, M. Kost, J. Sheridan, and M. C. Thompson, "Flow topology of a container train wagon subjected to varying local loading configurations," *Journal of Wind Engineering and Industrial Aerodynamics*, vol. 169, pp. 12–29, Oct. 2017, doi: 10.1016/j.jweia.2017.06.011.

[7] D. Flynn, H. Hemida, and C. Baker, "On the effect of crosswinds on the slipstream of a freight train and associated effects," *Journal of Wind Engineering and Industrial Aerodynamics*, vol. 156, pp. 14–28, Sep. 2016, doi: 10.1016/j.jweia.2016.07.001.

[8] F. Alam and S. Watkins, "Effects of Crosswinds on Double Stacked Container Wagons," Gold Coast, Australia, Dec. 2007.

[9] S. Giappino, D. Rocchi, P. Schito, and G. Tomasini, "Cross wind and rollover risk on lightweight railway vehicles," *Journal of Wind Engineering and Industrial Aerodynamics*, vol. 153, pp. 106–112, Jun. 2016, doi: 10.1016/j.jweia.2016.03.013.

[10] A. Kocoń and A. Flaga, "Critical velocity measurements of freight railway vehicles roll-over in wind tunnel tests as the method to assess their safety at strong cross winds," in *Journal of Wind Engineering and Industrial Aerodynamics*, Elsevier B.V., Apr. 2021. doi: 10.1016/j.jweia.2021.104559.

[11] D. Soper, C. Baker, and M. Sterling, "Experimental investigation of the slipstream development around a container freight train using a moving model facility," *Journal of Wind Engineering and Industrial Aerodynamics*, vol. 135, pp. 105–117, Dec. 2014, doi: 10.1016/j.jweia.2014.10.001.
[12] M. Sterling, C. J. Baker, S. C. Jordan, and T. Johnson, "A study of the slipstreams of high-speed passenger trains and freight trains," *Proc Inst Mech Eng F J Rail Rapid Transit*, vol. 222, no. 2, pp. 177–193, 2008, doi: 10.1243/09544097JRRT133.
[13] S. Giappino, S. Melzi, and G. Tomasini, "High-speed freight trains for intermodal transportation: Wind tunnel study on the aerodynamic coefficients of container wagons," *Journal of Wind Engineering and Industrial Aerodynamics*, vol. 175, pp. 111–119, Apr. 2018, doi: 10.1016/j.jweia.2018.01.047.
[14] D. Soper, C. Baker, and M. Sterling, "An experimental investigation to assess the influence of container loading configuration on the effects of a crosswind on a container freight train," *Journal of Wind Engineering and Industrial Aerodynamics*, vol. 145, pp. 304–317, 2015, doi: 10.1016/j.jweia.2015.03.002.
[15] M. Bocciolone, F. Cheli, R. Corradi, S. Muggiasca, and G. Tomasini, "Crosswind action on rail vehicles: Wind tunnel experimental analyses," *Journal of Wind Engineering and Industrial Aerodynamics*, vol. 96, no. 5, pp. 584–610, May 2008, doi: 10.1016/j.jweia.2008.02.030.
[16] D. Soper and C. Baker, "A full-scale experimental investigation of passenger and freight train aerodynamics," *Proc Inst Mech Eng F J Rail Rapid Transit*, vol. 234, no. 5, pp. 482–497, May 2020, doi: 10.1177/0954409719844431.
[17] D. Soper *et al.*, "Full scale measurements of train underbody flows and track forces," *Journal of Wind Engineering and Industrial Aerodynamics*, vol. 169, pp. 251–264, Oct. 2017, doi: 10.1016/j.jweia.2017.07.023.
[18] S. Wang, J. R. Bell, D. Burton, A. H. Herbst, J. Sheridan, and M. C. Thompson, "The performance of different turbulence models (URANS, SAS and DES) for predicting high-speed train slipstream," *Journal of Wind Engineering and Industrial Aerodynamics*, vol. 165, pp. 46–57, Jun. 2017, doi: 10.1016/j.jweia.2017.03.001.
[19] S. Wang, J. R. Bell, D. Burton, A. H. Herbst, J. Sheridan, and M. C. Thompson, "The performance of different turbulence models (URANS, SAS and DES) for predicting high-speed train slipstream," *Journal of Wind Engineering and Industrial Aerodynamics*, vol. 165, pp. 46–53, 2017.
[20] S. Maleki, D. Burton, and M. C. Thompson, "Assessment of various turbulence models (ELES, SAS, URANS and RANS) for predicting the aerodynamics of freight train container wagons," *Journal of Wind Engineering and Industrial Aerodynamics*, vol. 170, pp. 68–80, Nov. 2017, doi: 10.1016/j.jweia.2017.07.008.
[21] E. Principe, *Il Veicolo Ferroviario*. Roma: Collegio Ingegneri Ferroviari Italiani, 2010.
[22] C. Baker *et al.*, *Train Aerodynamics: Fundamentals and Applications*. Cambridge: Butterworth-Heinemann, 2019.
[23] J. Östh and S. Krajnović, "A study of the aerodynamics of a generic container freight wagon using Large-Eddy Simulation," *J Fluids Struct*, vol. 44, pp. 31–51, Jan. 2014, doi: 10.1016/j.jfluidstructs.2013.09.017.